UNPUBLISHED PRELIMINARY DATA

03424-10-T

THE UNIVERSITY OF MICHIGAN

78p.

N64-16763
CODE-1
CR-53112

COLLEGE OF ENGINEERING

DEPARTMENT OF NUCLEAR ENGINEERING
LABORATORY FOR FLUID FLOW AND HEAT TRANSPORT PHENOMENA

Technical Report No. 10

Cavitation Damage Measurements in Mercury by Radiotracer Analysis

OTS PRICE
XEROX $ 1.60 pb
MICROFILM $ 2.52 mf

WILLY SMITH
JUAN M. NIETO
FREDERICK G. HAMMITT

Under contract with:

National Aeronautics and Space Administration
Grant No. NsG-39-60
Washington, D. C.

Administered through:

October 1963

OFFICE OF RESEARCH ADMINISTRATION · ANN ARBOR

1539451 THE UNIVERSITY OF MICHIGAN U., Ann Arbor

COLLEGE OF ENGINEERING
Department of Nuclear Engineering

(2) Laboratory for Fluid Flow and Heat Transport Phenomena

Technical Report No. 10

CAVITATION DAMAGE MEASUREMENTS IN MERCURY BY RADIOTRACER ANALYSIS

Willy Smith,
Juan M. Nieto, and
Frederick G. Hammitt Oct. 1963 78p refs

ORA PROJECT 03424

under contract with:

NATIONAL AERONAUTICS AND SPACE ADMINISTRATION
(NASA GRANT NO. NsG-39-60; ORA Proj. 03424)
WASHINGTON, D. C.

[2]
[X] OTS

(NASA CR-53112; Rept. 03424-10-T) OTS: $7.60 ph, $2.54 mf

administered through:

OFFICE OF RESEARCH ADMINISTRATION ANN ARBOR

October, 1963

16763

ABSTRACT

A

The development of a method of continuous measurement of the wear of metal specimens submitted to a constant cavitation field by using radiotracer techniques was attempted. Samples of type 302 stainless steel and type 1010 carbon steel were irradiated in a nuclear reactor and then placed in a cavitating venturi in a closed-loop mercury facility.

It was discovered that due to the arrangement of the centrifugal pump, the radioactive particles of steel separate at once and tend to be trapped on the liquid surface of the pump sump. By dismantling this sump, about 6% of the measured weight loss of the carbon steel specimens was recovered. This radioactive material was collected and filtered, which allowed a classification by size with the following results: 68.95% of the material was retained on a 53 micron filter, 30.75% was retained on a 10 micron filter, and 0.307% was retained on a 2 micron filter. These results were obtained by comparison of the activity of the debris with the activity of a standard sample prepared from the original irradiated specimen.

Differential curves obtained for the different size debris indicate that the constituents do not vary with particle size. On the assumption that the particles are spheres, it was found that the size distribution of the debris recovered was as follows: 6000 particles with a diameter of 53 microns, 14,750 with an average diameter of 30 microns, and 18,400 with an average diameter of 6 microns. Very few particles exceed a diameter of 80 microns (3.15 mils) and very few have a dimension of less than 6 microns (.236 mils).

AUTHOR

ACKNOWLEDGMENTS

The authors express their gratefulness for the valuable assistance received from Mr. M. John Robinson, Research Assistant in the Nuclear Engineering Department, who operated the test facility, Mr. Larry Barinka, who assisted in the test, and Mr. John Jones, of the Radiation Control Service, who collaborated in the preparation and handling of the radioactive specimens.

TABLE OF CONTENTS

	Page
ABSTRACT	ii
ACKNOWLEDGMENTS	iii
LIST OF FIGURES	vi
LIST OF TABLES	viii
I. INTRODUCTION	1
A. Motivation for the Investigation	1
B. Description of the Facility	3
C. Review of Previous Water Tests	6
II. EXPERIMENTAL PROCEDURE	10
A. Irradiation of Test Specimens	10
1. Required Irradiation	10
2. Maximum Allowable Irradiation	11
3. Irradiation Properties of Test Materials	12
4. Estimates of Activity and Dose Rate	15
B. Facility Additions	19
C. Stainless Steel Specimen Experimental Run	22
1. General	22
2. Filtration Procedure	23
3. Mercury Activity Measurement	26
D. Carbon Steel Specimen Experimental Run	27
1. General	27
2. Recovery and Counting of Radioactive Debris	30
III. RESULTS AND DISCUSSION OF CARBON STEEL TEST	33
A. General	33
B. Mass of Debris Recovered and Particle Size Distribution	36
C. Correlation With Visual Pit Counting	40
D. Relative Constituents of Debris vs. Original Specimen	42
IV. CONCLUSIONS	42
A. General Feasibility of Method	42
B. Particular Experimental Results	43
BIBLIOGRAPHY	45

TABLE OF CONTENTS (CONTINUED)

	Page
APPENDIX.	46
A. Estimate of Stainless Steel Specimen Activity. . .	47
B. Estimate of Activity of Mercury Samples.	53
C. Calibration in Energy of the MCA	55
D. Evaluation of the Area Under the Photopeak	55
E. Mass of Debris Recovered and Particle Size Distribution	59
1. Debris Recovered.	59
2. Particle Size Distribution.	67

LIST OF FIGURES

Figure		Page
1	Cross Section of Cavitating Venturi.	4
2	Photograph of Test Specimen.	5
3	Overall Loop Schematic	7
4	Schematic of Pump Arrangement.	8
5	Decay Scheme of Ni^{65} (Ref. 12)	16
6	Decay Scheme of Fe^{59} and Mn^{56} (Ref. 11).	17
7	Decay Scheme of Cr^{51} and Co^{60} (Ref. 9)	18
8	Partial View of Cavitation Loop Showing the Arrangements Made to Take Liquid Samples From Main Stream and Sump.	20
9	Other View of the Modifications Added to the Mercury Loop.	20
10	Photograph of the Filtering Arrangement.	21
11	Cross Section of Filtering Rack.	24
12	Differential Curve of Stainless Steel Specimen	28
13	Differential Curves of Debris Retained by the Different Pore Size Filters.	32
14	Differential Curve of Carbon Steel Specimen	34
15	Percent Weight of Steel Passing Through Filters vs. Filter Pore Size	39
16	Photomicrograph of Carbon Steel Specimen Prior to Irradiation and Cavitation Damage.	41
17	Photomicrograph of Irradiated Carbon Steel Specimen After 50 Hours of Standard Cavitation.	41
	APPENDIX	
1A	Differential Curves of Co^{60}, Cs^{137} and Na^{22}.	56
2A	Calibration Curve for MCA: channel number versus Gamma-ray Energy	57
3A	Photopeak for Gaussian Distribution About Gamma-ray Energy.	58

LIST OF FIGURES (CONTINUED)

Figure		Page
4A	1.10 Mev Photopeak of Fe^{59} in Calibrated Sample. . . .	61
5A	1.10 Mev Photopeak of Fe^{59} Retained on 53 Micron Filter.	63
6A	1.10 Mev Photopeak of Fe^{59} Retained on 10 Micron Filter	64
7A	1.10 Mev Photopeak of Fe^{59} Retained on 2 Micron Filter	66

LIST OF TABLES

Table		Page
I	Elements Present in 302 Stainless Steel Tested.	13
II	Nuclear Properties of the Isotopes Present in 302 Stainless Steel After Irradiation	14
III	Filtration Schedule for Stainless Steel Run	23
IV	Weights of Carbon Steel Specimens (grams)	33
V	Mass and Size Distribution of the Particles Recovered on the Different Filters.	37
VI	Comparison of Number of Pits Observed With Number of Particles of Similar Size in the Debris.	40

APPENDIX

I-A	Estimate of Activities of the More Important Isotopes Contained in the Stainless Steel Specimens . . .	50
II-A	Values of the Specific Radiation Flux R_o For The Isotopes of Interest.	52
III-A	Estimated Dose Rates for Stainless Steel Specimens. . . .	53
IV-A	Percentage of Debris Retained and Passing Through the Different Filters.	67

I. INTRODUCTION

A. Motivation For The Investigation

Cavitation damage or erosion investigations are always hampered, and especially so when the fluids utilized are under elevated temperature or are such that severe technological handling problems are involved, by the difficulty of measuring the quantity of damage incurred. In the case of high-temperature liquid metals, which are of special interest to the present investigation, the difficulties associated with the removal and examination of damage specimens may be severe. Hence the development of a technique for measuring such damage without actual disassembly and shut-down of equipment is extremely desirable.

A technique having considerable apparent potential for the attainment of such measurements is the use of irradiated test specimens combined with a radioactivity measurement of the process stream. Conceivably, in such a manner, an instantaneous measure of wear-rate could be obtained without stopping the test or removing the specimens, and thus an accurate determination of wear-rate as a function of time could be obtained easily, a precision measurement not readily achieved otherwise even in water tests. Additional valuable data also would appear to be attainable from such tests:

i) Measurement of damage-debris size spectrum, by passing debris through precision filters and counting the radioactivity remaining on the filters.

ii) Measurement of relative proportions of constituents in damage debris, and comparison with those of parent material, to determine whether or not attack is selective.

A previous experiment under the present cavitation damage investigation was conducted using an irradiated austenitic stainless steel test specimen in water[1,2]. While the experiment was rather crude, and was partially in the nature of a feasibility test, the results were surprisingly favorable. The resulting damage vs. time determination was everywhere proportional to data computed from actual pit counts[1,2,3,4], although the absolute magnitudes were in considerable error. In addition a particle-size determination was achieved that agreed within the known experimental errors with the microscopic observations of the damaged surfaces.

In view of the relatively substantial initial success achieved with water, it was decided to procede with the development of the technique by attempting a similar experiment in mercury, using somewhat more elaborate radiation instrumentation, and hoping to achieve more precise measurements which would be of significance in themselves, and also would contribute toward the development of a technique which could be used in high-temperature liquid metals.

As related in detail in reference 5 and more briefly in the body of this report, some success was achieved particularly in the areas of determination of relative proportions of constituents in damage debris, and in measuring particle size distribution. In the second instance, even though the measurements are somewhat crude, they are unique at present for this type of test in a liquid metal (as the measurements from the water experiment were and still are, to the authors' knowledge, for that fluid), and hence are of significant value. It is believed that the measurement of relative constituents,

which was not achieved in the water tests, is more precise, and is also unique at present.

In addition, the experiment has succeeded in pin-pointing some of the major problems involved in the general use of these techniques, particularly for relatively unknown fluids and flow geometries. The difficulties encountered involve principally filtering of various fluids (non-wetting, high melting point, chemically active, toxic, etc.) and maintaining a uniform concentration of the debris in the process and filtering streams.

B. Description of the Facility

The previous as well as the present experiments were carried out in the mercury tunnel facility described in detail in the references already cited. The most significant features from the viewpoint of these particular experiments will be summarized here for convenience.

Cavitation is caused to occur in a transparent (plexiglass) venturi of approximately 0.5 inches cylindrical throat diamater (Figure 1), and damage is observed on two small tapered test specimens (Figure 2), inserted parallel to the flow through the wall of the diffuser section. By suitable adjustment of the pressures and flow, the apparent termination of the vaporous cavitation region can be caused to occur approximately at the axial midpoint of the specimens, as it was in these tests ("Standard Cavitation" in the terminology of these experiments). The throat velocity is an independent variable within a certain range, and it was set at $\sim$70 ft./sec. for the earlier water tests and $\sim$34 ft/sec. for the present mercury tests. Under these conditions the mean fluid transit time around the loop is of the order 5-15 seconds, and the Reynolds' number at all points is in the highly

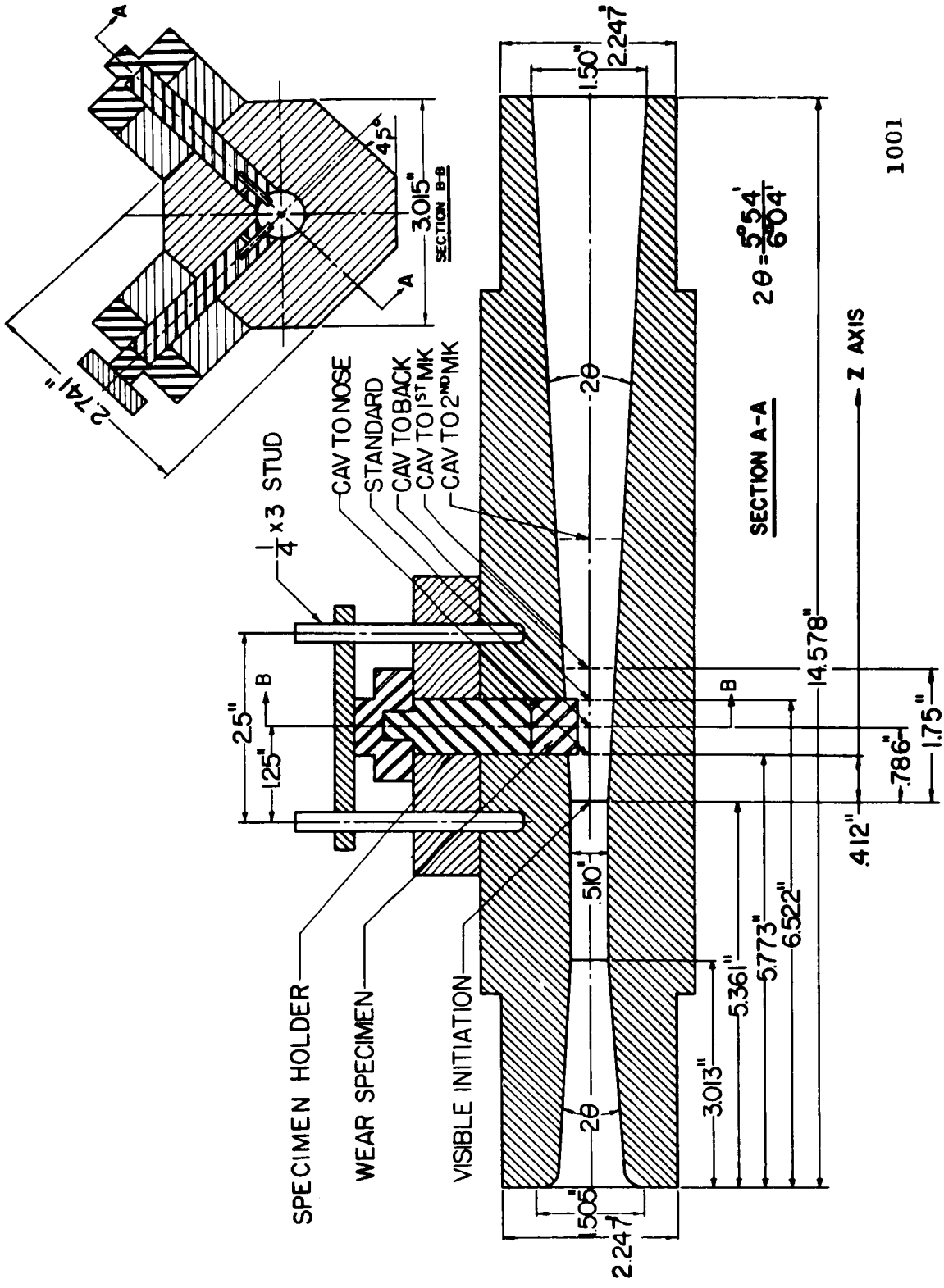

Figure 1. Cross Section of Cavitating Venturi.

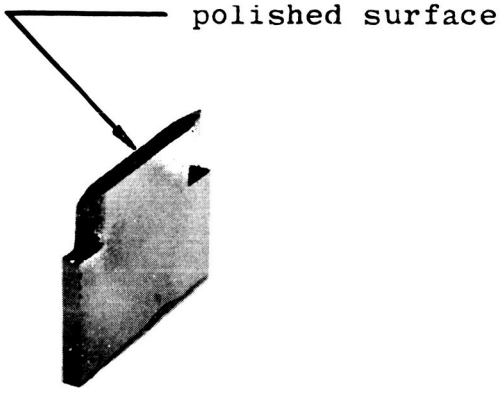

Figure 2. Photograph of Test Specimen.

turbulent range. Fluid temperature for both tests was approximately ambient.

The loop (Figure 3) is powered by an overhung centrifugal sump pump (Figure 4). In this arrangement there is a strong separating effect upon foreign matter of density less than that of the fluid, due to the centripetal action of the impeller, resulting in a tendency of such material to escape from the main stream into the sump, where it is trapped and floats to the surface of the liquid. This effect was particularly evident during the mercury tests. The fluid circulation in the sump is reduced to very little by a matrix of closely-packed vertical stainless steel rods.

C. Review of Previous Water Tests[1,2]

The test material used in the previous water tests, and also in the initial mercury test, was annealed type 302 stainless steel*. In the water test, the wear rate as calculated from the radioactivity count of the filters, ranged, as a function of time from test start, between 0.15 and 0.001 mg/hr., and the particle diameters were predominantly between 0.5 and 3 mils. These values were used to provide some rough idea of the filter gradations to be employed and of the required irradiation level for the test specimens, taking into account the fact observed in many previous damage tests that the damage rate for mercury may be as much as 100 times that of water, under otherwise similar test conditions.

Filtering in the water tests was accomplished using a filter rack (Figure 11) accomodating four 47 mm. diameter cloth or paper filters in series, inserted into a small by-pass stream from the loop

* Selected because a great deal of previous damage data in both water and mercury had been accumulated for this material.

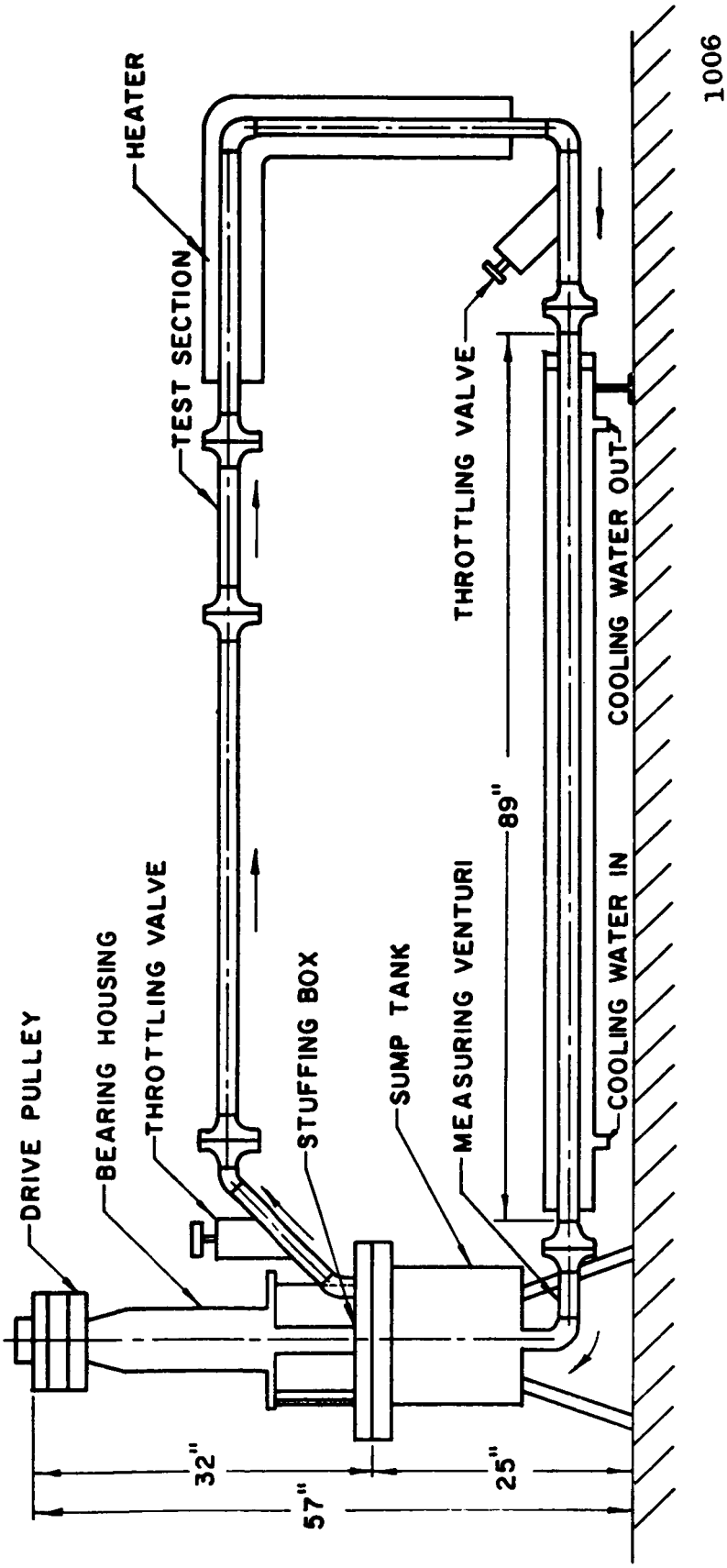

Figure 3. Overall Loop Schematic.

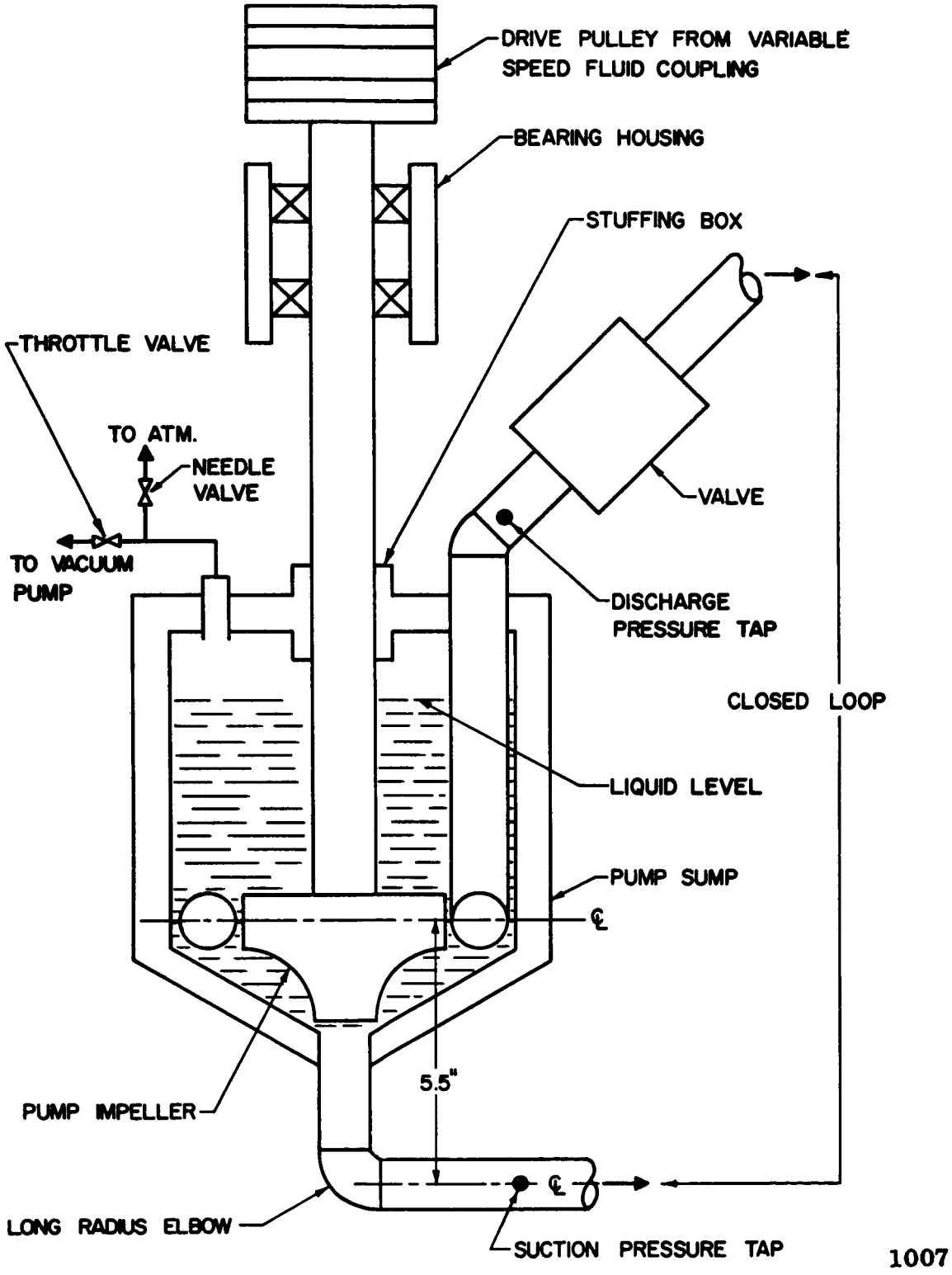

Figure 4. Schematic of Pump Arrangement.

in such a manner that all the water entering the filter system must pass through each filter.

A first run of 20 hours duration was made and each hour a 5 cc. water sample withdrawn from the loop into lucite thimbles. After the experiment was completed, the samples were evaporated on stainless steel planchets, and counted with a gas flow counter using an integral counting technique. At the conclusion of the test, part of the circulation water was by passed through the filter rack while the main circulating stream was held at full velocity to maintain agitation. Two runs were made with different sets of filters. Finally a third run was made with the main stream essentially stagnant using the same size filters as in the first run to determine whether settling rates and/or entrapment were significant. The activity of the filters was determined with a 2π gas-flow proportional counter. The relationship between milligrams of metal and counts per minute was determined by making a calibration with a standard solution, obtained by cutting a small piece from one of the radioactive specimens. The metal fragments were accurately weighed, and then dissolved in concentrated hydrochloric acid and diluted to three known concentrations.

The following results were obtained:

i) The highest wear rate observed during the 20 hours experiment was 0.15 mg/hr., and was recorded at the beginning of the run. After about 4 hours of cavitation, the damage had become much less severe (about 0.001 mg/hr.) and during the last 15 hours there was a gradual increase of the wear rate.

ii) Count-rate determinations of the filters indicated that more than 70% of the wear debris consisted of particles ranging from

0.5 to 3 mils in diameter, and only trace amounts were found smaller than 1 micron.

As discussed later, the gamma activity of the specimens is due not only to Fe 59, to which it was attributed in the initial water tests[1,2], but also to other isotopes which chemical analysis indicates are present in the specimens. However, since the activity of the filters was counted with a gas flow proportional counter, where actually the activity due to beta radiation was measured, the exact consideration of the gamma emitters present in the specimens was of no importance.

II. EXPERIMENTAL PROCEDURE

A. Irradiation of Test Specimens

1. Required Irradiation

An estimate of the required irradiation of the stainless steel test specimens for the mercury tests was made considering the following:

i) Anticipated rate of damage considering similar previous tests with non-irradiated specimens, but where weight loss had been measured.

ii) Minimum required activity level in mercury for good counting statistics assuming debris to be uniformly dispersed through the entire facility contents.

iii) Safety factors to account for likely errors in estimations including the previous mismatch between damage calculated from activity of filters in previous water tests and that estimated from pit counts.

iv) Irradiation properties of the stainless steel used (as discussed in further detail later).

The irradiation was to be obtained by inserting the specimens, in a sealed quartz tube, into the Ford Nuclear Reactor at this university (swimming pool, thermal, research reactor). Since this reactor is generally operated on a 5-day week, 8-hour day schedule, this intermittent irradiation, allowing an appreciable decay in the case of some of the isotopes during the down periods, as well as the varying flux levels during operation were considered in evaluating the required exposure time in the reactor[6]. The irradiation actually attained was of course verified by measuring the activity of the specimens, for reasons of safe-handling as well as verification of the calculations, before inserting them into the loop.

Further details on the estimation of activity as a function of reactor time is given in the appendix.

2. Maximum Allowable Irradiation

The maximum allowable irradiation is set by two factors:

i) Safe handling - It is difficult to place an absolute limit on the maximum specimen activity which can be safely handled. It is more a question of the provision of sufficiently elaborate, and perhaps expensive equipment for the handling. In the present case, the activity levels used were not sufficient to cause much difficulty on this score.

ii) Irradiation damage to test specimen - Too high an irradiation level will, of course, alter the physical properties of the material to be tested and thus destroy to some extent the significance of the test. Fortunately the limit for metallic materials in general is quite high, as compared, for example, to plastics, other organics, etc. According to the best available information[7, 8], stainles steel

undergoes no measurable change in mechanical properties as a result of neutron irradiation of less than 10^{18} nvt fast flux. The fast flux in the Ford Nuclear Reactor is about 5% of the thermal flux. It was then calculated that the stainless steel specimens for the mercury tests received about 1.5×10^{17} nvt fast flux, and the carbon steel specimens later tested about 0.5×10^{17} nvt fast flux. Thus in both cases no change in mechanical properties of the test materials should have occurred, but the margin for a further increase in irradiation is small. Hence it appears that irradiation damage, even for metals, is a more meaningful limit to maximum activity than is safety. This would very likely be increasingly so for non-metallic materials so that perhaps tests of the herein sort described would not be practical.

3. Irradiation Properties of Test Materials

Two test materials were utilized: type 302 stainless steel, and 1010 carbon steel. The initial test which was planned was that with stainless steel and considerably more care and preliminary analysis was used in this case than with the later test with carbon steel which was primarily, as will be explained in a later section, a feasibility test. Hence, a chemical analysis was obtained on a specimen of the stainless steel material to be used (the same stock which had been used in many previous non-irradiated damage tests), and considerable care was utilized in determining the nature of the radioactivity to be expected. The results of the chemical and spectrographic analysis of the stainless steel are listed in Table I.

TABLE I

Elements Present in 302 Stainless Steel Tested*

Iron	68.39%	Phosphorous	0.010%
Chromium	18.35%	Tellurium	Not Analyzed
Nickel	10.72%		
Silicon	0.68%	Titanium	Not Detected
Manganese	1.28%	Aluminum	Not Detected
Molybdenum	0.21%	Tungsten	Not Detected
Copper	0.25%	Vanadium	0.04%
Columbium	Not Detected	Cobalt	0.03%
Tin	0.04%	Magnesium	Not Detected
Selenium	Not Analyzed	Zirconium	Not Detected

For purposes of estimating activity to be expected after irradiation and dose rate, an average specimen weight of 3.2 grams was used.

The complete analysis of the nuclear properties of the different isotopes present in the stainless steel samples is summarized in Table II. In column one the different isotopes present in the steel prior to irradiation are listed. The natural abundance (a %) of each is listed in column two[9]. Column three gives the percentage of the element (b %) in the specimen from the chemical analysis. In column four the atomic weight (W) of the natural elements are given.[9]

The number of atoms per gram of sample, N (fifth column), is calculated using the formula,

$$N = \frac{N_o}{W} \quad \frac{ab}{10^4}$$

where No is Avogadro's number, 6.025×10^{23} atoms/atom-gram.

---

* Analyzed by The Detroit Testing Laboratory, Inc.

Line	Isotope	Natural Abundance	b%	W Atomic weight	N atoms / cm sample	σ_a barns	Isotope formed	Type of decay	Beta Energy Mev	Gamma Energy Mev	Half-life $T_{\frac{1}{2}}$	λ hr^{-1}
1	Fe-54	5.84	68.39	55.85		2.8	Fe-55	EC		no γ	2.94 y	
2	Fe-56	91.68				2.6	Fe-57	γ		0.014	10^{-7}s	
3	Fe-57	2.17				2.5	Fe-58	stable				
4	Fe-58	0.31			2.29×10^{19}	1.01	Fe-59	β^-, γ	.271(46%) .462(54%) 1.56(.3%)	.191(2.8%) 1.098(57%) 1.289(43%)	45.1d	6.41×10^{-4}
5	Mn-55	100	1.28	54.94	1.405×10^{20}	13.3	Mn-56	β^-, γ	2.81(50%) 1.04(30%) 0.65(20%)	.845(100%) 1.76(30 %) 2.17(20 %)	2.59h	0.27
6	Si-28	92.27	0.68	28.09		0.08	Si-29	stable				
7	Si-29	4.68				0.28	Si-30	stable				
8	Si-30	3.05				11×10^{-2}	Si-31	β^-, γ	1.471	1.26(.07%)	2.62h	
9	Cr-50	4.31	18.35	52.01	9.15×10^{19}	15.9	Cr-51	EC, γ		.325(9 %)	27.9 d	1.035×10^{-3}
10	Cr-52	83.76				0.76	Cr-53	stable				
11	Cr-53	9.55					Cr-54	stable				
12	Cr-54	2.38				0.38	Cr-55	β^-	2.85		3.6 m	
13	Ni-58	67.76	10.72	58.71		4.20	Ni-59	EC			10^5 y	
14	Ni-60	26.16					Ni-61	stable				
15	Ni-61	1.25					Ni-62	stable				
16	Ni-62	3.66				15	Ni-63	β^-	0.067			
17	Ni-64	1.16			1.277×10^{19}	1.52	Ni-65	β^-, γ	2.10(69%) 1.01(8 %) 0.60(23%)	1.49(18.8%) 1.12(12.9%) 0.37(4.9%)	2.56h	0.27
18	P-31	100	0.01	30.975		0.19	P-32	β^-	1.707		14.22d	
19	Cu-63	69.1	0.25	63.75		4.51	Cu-64	EC, β^+, β^-	.571, 0.65	1.35(.5%)	12.80h	
20	Cu-65	30.9				1.80	Cu-66	β^-, γ	several	several	5.10 m	
21	Mo-92	15.86	0.21	95.95		$<6 \times 10^{-3}$	Mo-93	EC			> 2 y	
22	Mo-94	9.12					Mo-95	stable				
23	Mo-95	15.70					Mo-96	stable				
24	Mo-96	16.50					Mo-97	stable				
25	Mo-97	9.45					Mo-98	stable				
26	Mo-98	23.75				0.51	Mo-99	β^-, γ	several	several	66 h	
27	Mo-100	9.62				0.20	Mo-101	β^-, γ	several	several	14.61m	
28	Sn-112	0.95	0.04	118.7		1.3	Sn-113	EC,		0.392	119 d	
29	Sn-114	0.65					Sn-115	stable				
30	Sn-115	0.34					Sn-116	stable				
31	Sn-116	14.24				6×10^{-3}	Sn-117	stable				
32	Sn-117	7.57					Sn-118	stable				
33	Sn-118	24.01				10×10^{-3}	Sn-119	stable				
34	Sn-119	8.58					Sn-120	stable				
35	Sn-120	32.97					Sn-121	β^-	0.383		27.5 h	
36	Sn-122	4.71					Sn-123	β^-, γ	1.260	0.153	39.5 m	
37	Sn-124	5.98				0.2	Sn-125	β^-, γ	several	several		
38	Co-59	100	0.03	58.94	3.07×10^{18}	20 ± 3	Co-60	β^-, γ	0.312	1.17, 1.33	5.24y	1.5×10^{-5}
39	Va-50	0.25	0.04	50.95			Va-51	stable				
40	Va-51	99.75				4.5	Va-52	β^-, γ	2.470	1.44	3.76 m	
	(1)	(2)	(3)	(4)	(5)	(6)	(7)	(8)	(9)	(10)	(11)	(12)

TABLE II. Nuclear Properties of the Isotopes Present in 302 Stainless Steel After Irradiation.

In column six, the thermal absorption cross sections, σ_a, in barns, are given[10].

The isotopes formed after irradiation are indicated in column seven, while the type of decay is indicated in column eight. The energy of the radiation emitted expressed in Mev is given in columns nine and ten. The half-life of the unstable isotopes appears in column eleven, and finally the decay-constants (hrs^{-1}) are given in column twelve.

Before proceeding to calculate the activity produced by these unstable isotopes, we eliminate those which are of no interest because of one or more of the following reasons:

a) very short half-life (minutes or less)

b) very large half-life (more than 10^2 years)

c) pure beta-emitters

d) the product ab is very small.

When this is done, the forty initial possibly important radioactive isotopes reduce to five: Fe-59, Mn-56, Cr-51, Ni-65, and Co-60. For the case of Cr-51 in particular, the decay takes place by electron capture, which in 9% of the cases, is followed by a gamma ray of .325 Mev. In 91% of the cases, the EC leads to the ground state of V-51 with an end-point energy for the internal bremsstrahlung of 0.75 Mev[11]. The decay schemes of the five isotopes mentioned above are shown in Figures 5, 6, and 7.

4. Estimates of Activity and Dose Rate

Detailed theoretical estimates of activity and dose rate were made as a function of reactor flux, exposure time, and reactor schedule for the stainless steel specimens, and from these the desired

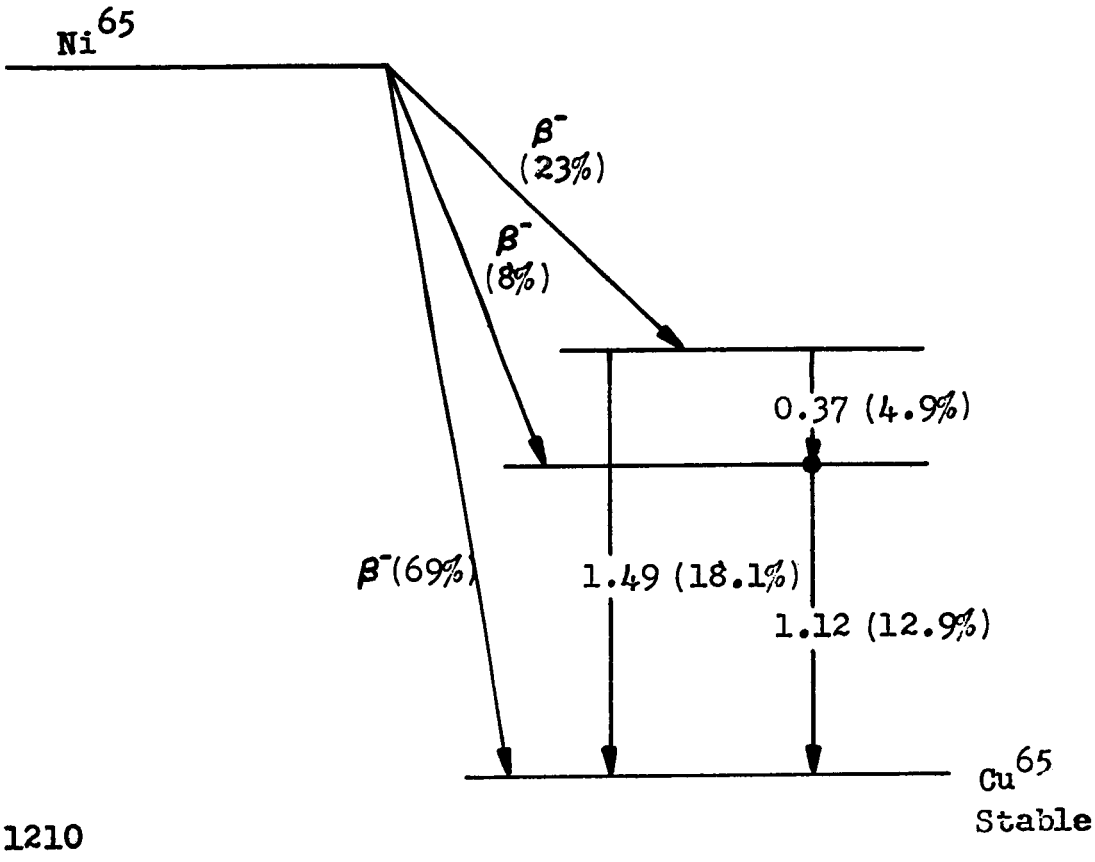

Figure 5. Decay Scheme of Ni^{65} (Ref. 12).

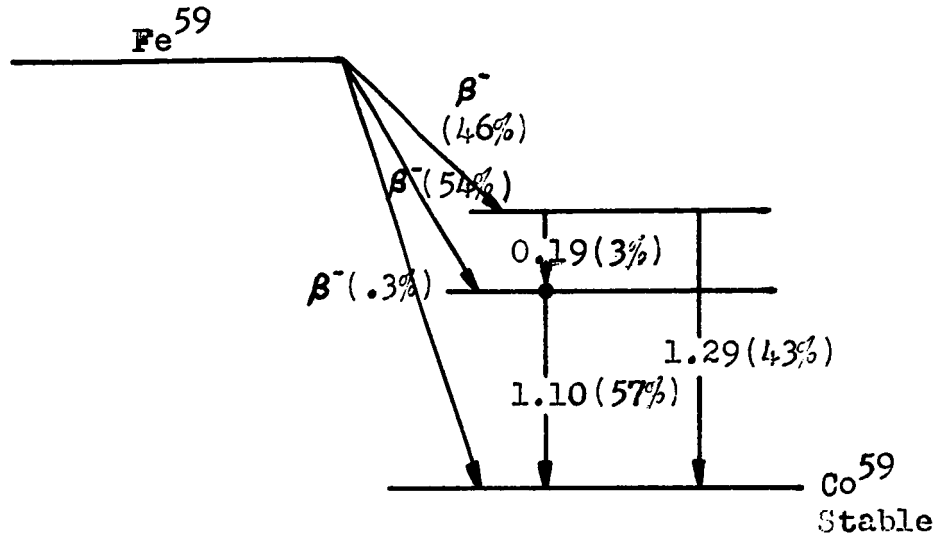

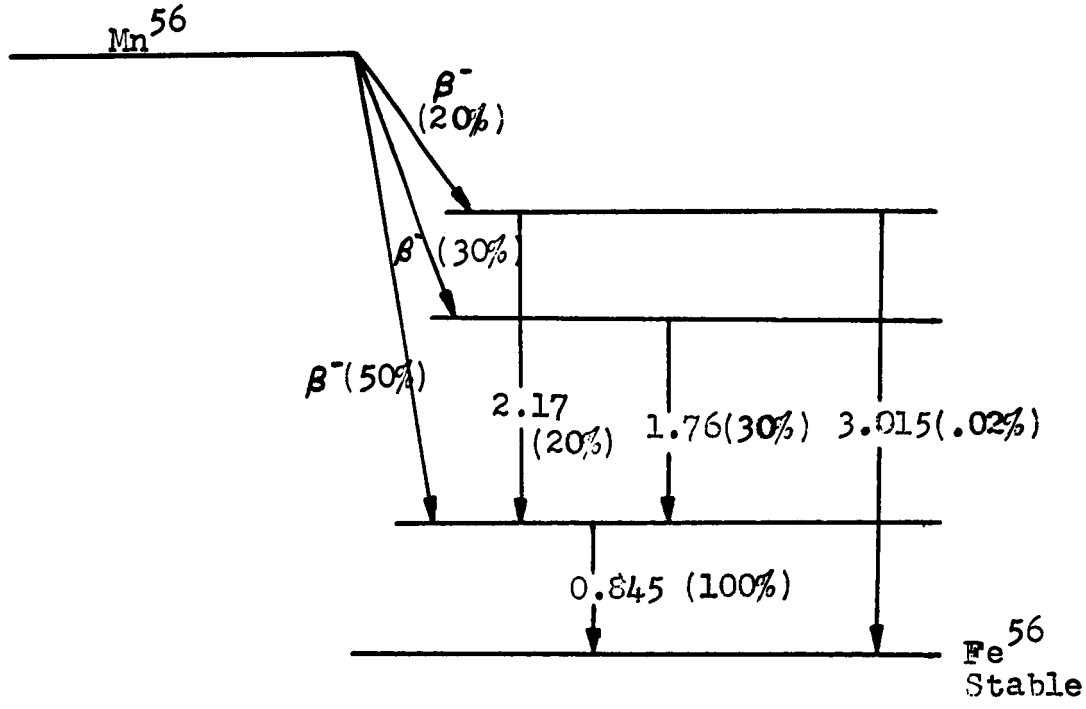

1208

Figure 6. Decay Scheme of Fe^{59} and Mn^{56} (Ref. 11).

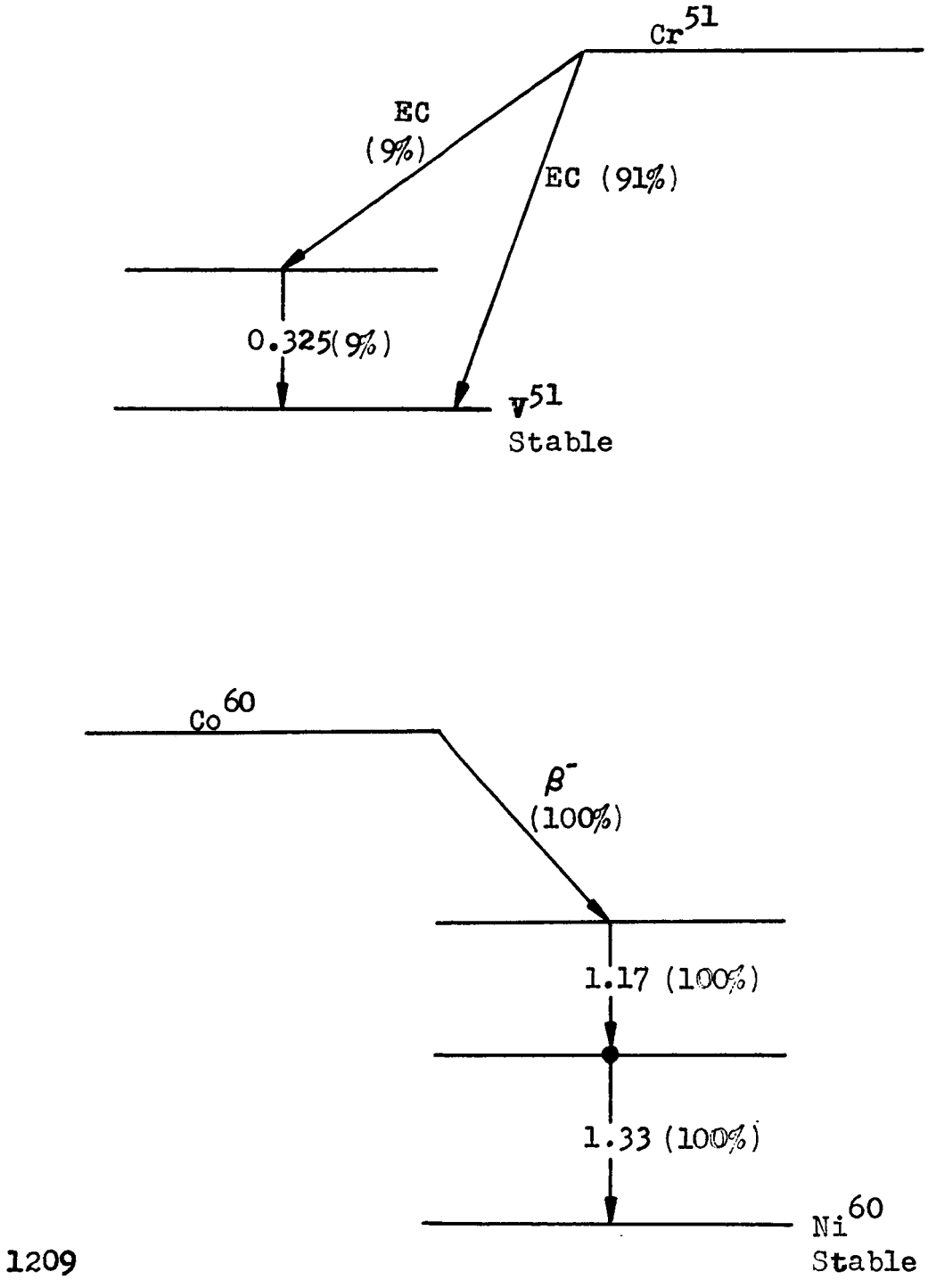

Figure 7. Decay Scheme of Cr^{51} and Co^{60} (Ref. 9).

exposure in the reactor was scheduled, necessary to achieve the required activity and dose rate in the mercury samples to be utilized. The details of these calculations are given in Sections A and B of the Appendix.

B. Facility Additions

In order to make liquid samples from the main stream and from the sump of the facility, two new taps were required as shown in Figures 8 and 9 where they are designated A and C. Tap C allowed samples of mercury to be taken from the main stream and tap A from the sump, B. The arrangement for returning the liquid samples to the loop after filtration is also shown. With tap D closed, samples were put through the funnel, G, and by opening the tap, F were allowed to proceed to the container, E. Once the container was full of mercury, tap F was closed and by opening the tap, I, shop air was allowed to enter container, E. The opening of tap D then forced the mercury back to the main stream through the tubing, H. Figure 10 shows the arrangement by which the filtering process was performed. The samples which had been removed as described before, from the main stream and from the sump, were poured through funnel A into the container D, while taps C and F were closed, and tap B open. Once the mercury was in container D, tap B was closed and tap C was opened, allowing shop air pressure to enter. The opening of tap F permitted the mercury to be forced through the filter rack, E. Four filters of varying mesh size can be used simultaneously in this apparatus, which is described in the next section.

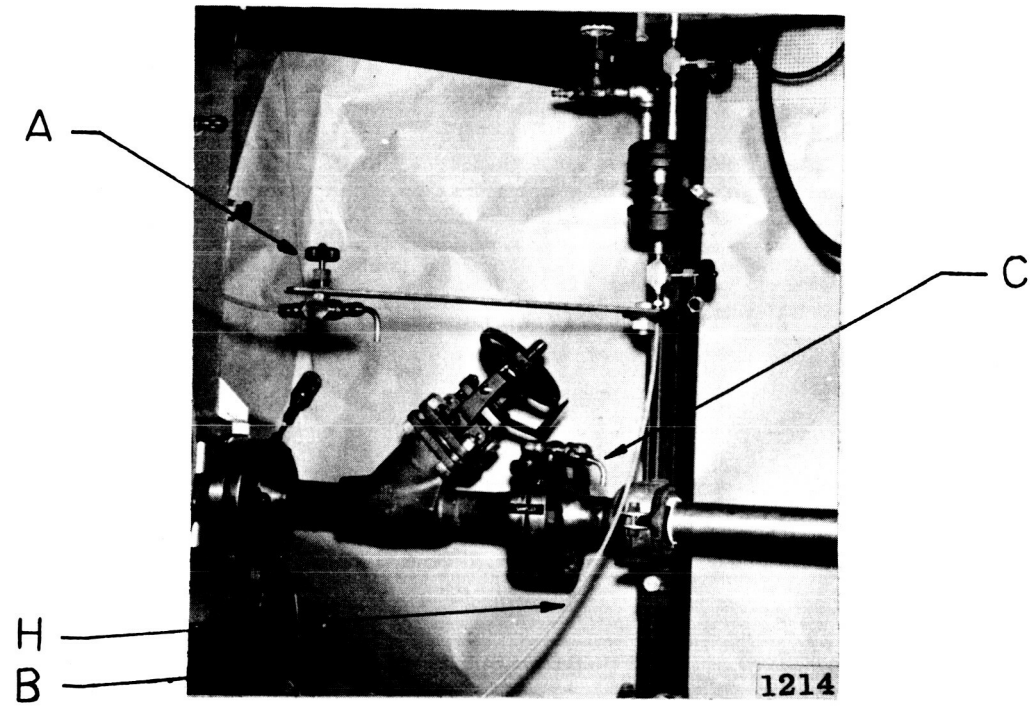

Figure 8. Partial View of Cavitation Loop Showing the Arrangements Made to Take Liquid Samples From Main Stream and Sump.

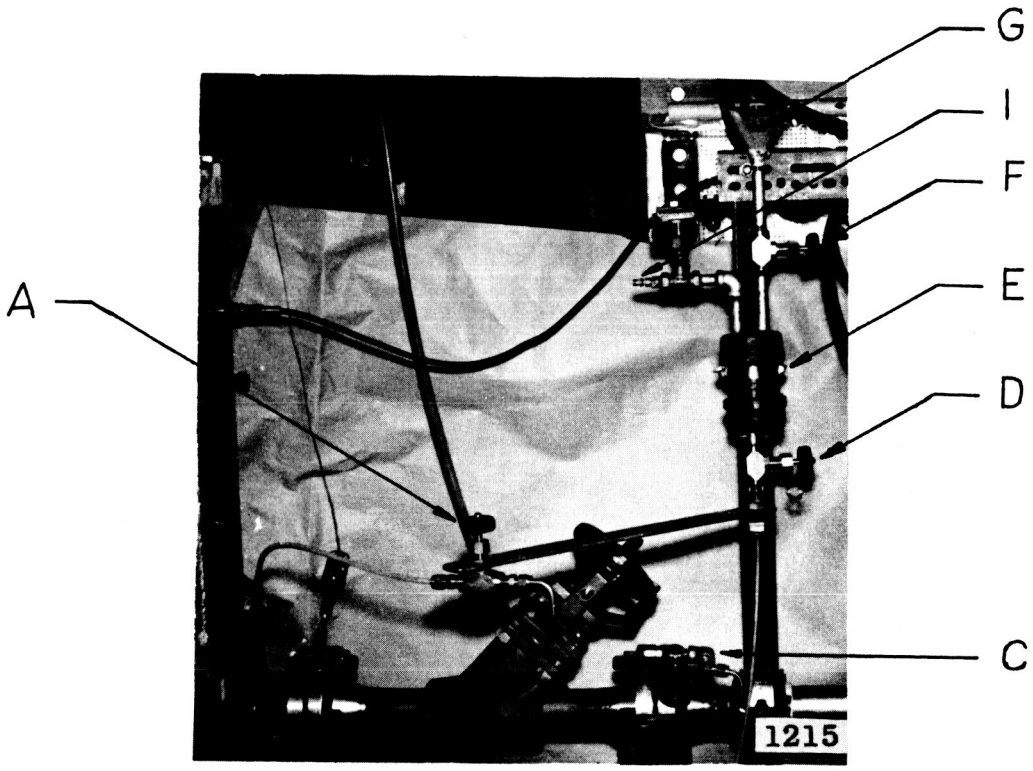

Figure 9. Other View of the Modifications Added to the Mercury Loop.

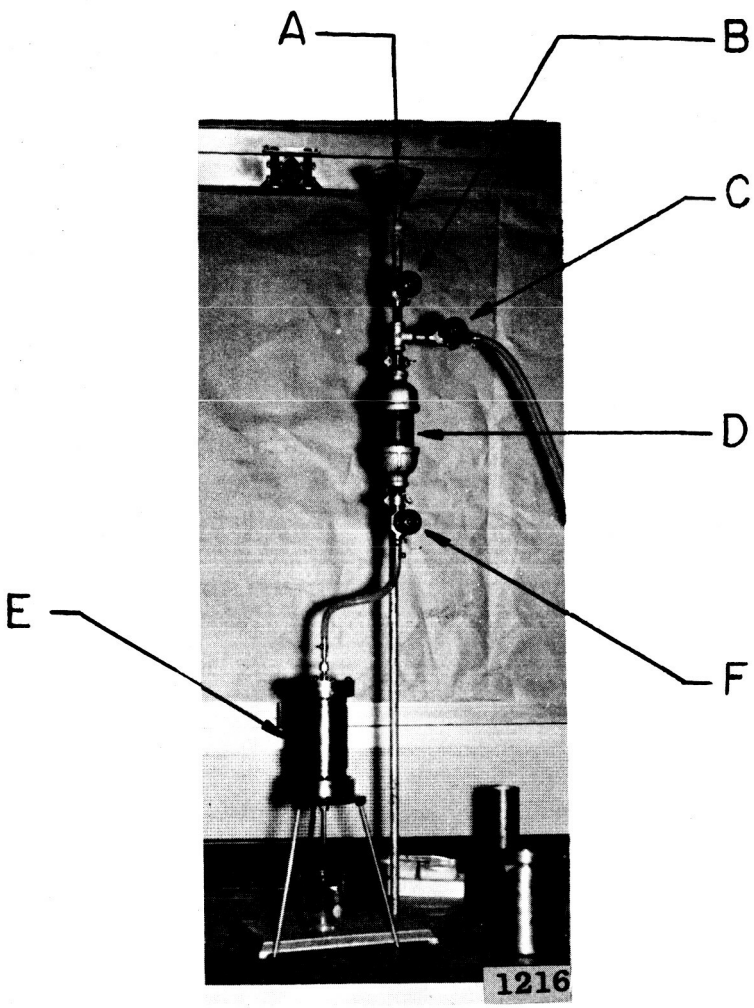

Figure 10. Photograph of the Filtering Arrangement.

C. Stainless Steel Specimen Experimental Run

1. General

Two type 302 annealed stainless steel specimens were used in the first run. Although no direct weight loss measurement was obtained*, they were observed under a metallographic microscope after the test, and it was ascertained that their appearance was about that of non-irradiated specimens of the same material which had been previously run for similar cavitation tests, and for which an average weight loss of 1.2 mg per specimen had been measured. This weight loss was then taken as the basis for further order of magnitude calculations.

The irradiation of the two specimens was accomplished with a total reactor on-time of 172.5 hours. (The chronological time was much longer - about 1000 hours). This irradiation period corresponds more or less to a value of n = 20 days, according to the calculation made in Reference 6. The actual activity attained was much less than that previously estimated. The dose rate of the two specimens was measured approximately 24 hours after the end of irradiation, giving 5 r/hr on bare contact (vs. 45 r/hr. estimated at 1 cm. -- Table III-A), and 10 mr/hr. through the casket shielding.

The run was made over a continuous duration of 26 hours. "Standard Cavitation" ** was used with a throat velocity of $\simeq$ 34 ft./sec.

---

* An initial weight had been obtained, but a final weighing was inadvertently neglected until the specimens had been destroyed to obtain samples for radiation characteristic measurements.

** When the visual termination of the cavitation region occurs at the axial midpoint of specimens.

2. Filtration Procedure

Samples were taken according to the schedule shown in Table III from two locations in the loop: (i) from the sump, and designated by 1S, 2S, etc.; and (ii) from the loop main stream, designated 1L, 2L, etc. As shown in the table, they were taken quite frequently at first since, based on previous tests, it was known that the initial damage rate would be quite high.

TABLE III

Filtration Schedule For Stainless Steel Run

Duration Interval	Frequency	Location	No. Filters
0 to 2 hrs.	15 min.	Loop, Sump	Single
2 to 6 hrs.	30 min.	Loop, Sump	Single
6 to 12 hrs.	60 min.	Loop, Sump	Single
12 to 26 hrs.	120 min.	Loop, Sump	Single

In addition, eight samples for multiple filtration were taken; four from the loop and four from the sump, at the following times: t = 15 min.; 2 hr. and 15 min.; 6 hrs. and 15 min.; and 8 hrs. and 15 min.

The cross section of filtering rack used is shown in Figure 11. The filter discs are arranged in series and sealed around the periphery by the axial load imposed by the closing bolts. The relatively flimsy filter discs (cloth or paper) are backed-up by steel discs with numerous small holes to prevent tearing. This apparatus was previously used in the water tests[1,2] and performed successfully.

Preliminary trials at filtering mercury in the same apparatus were made prior to the actual test run. It was soon

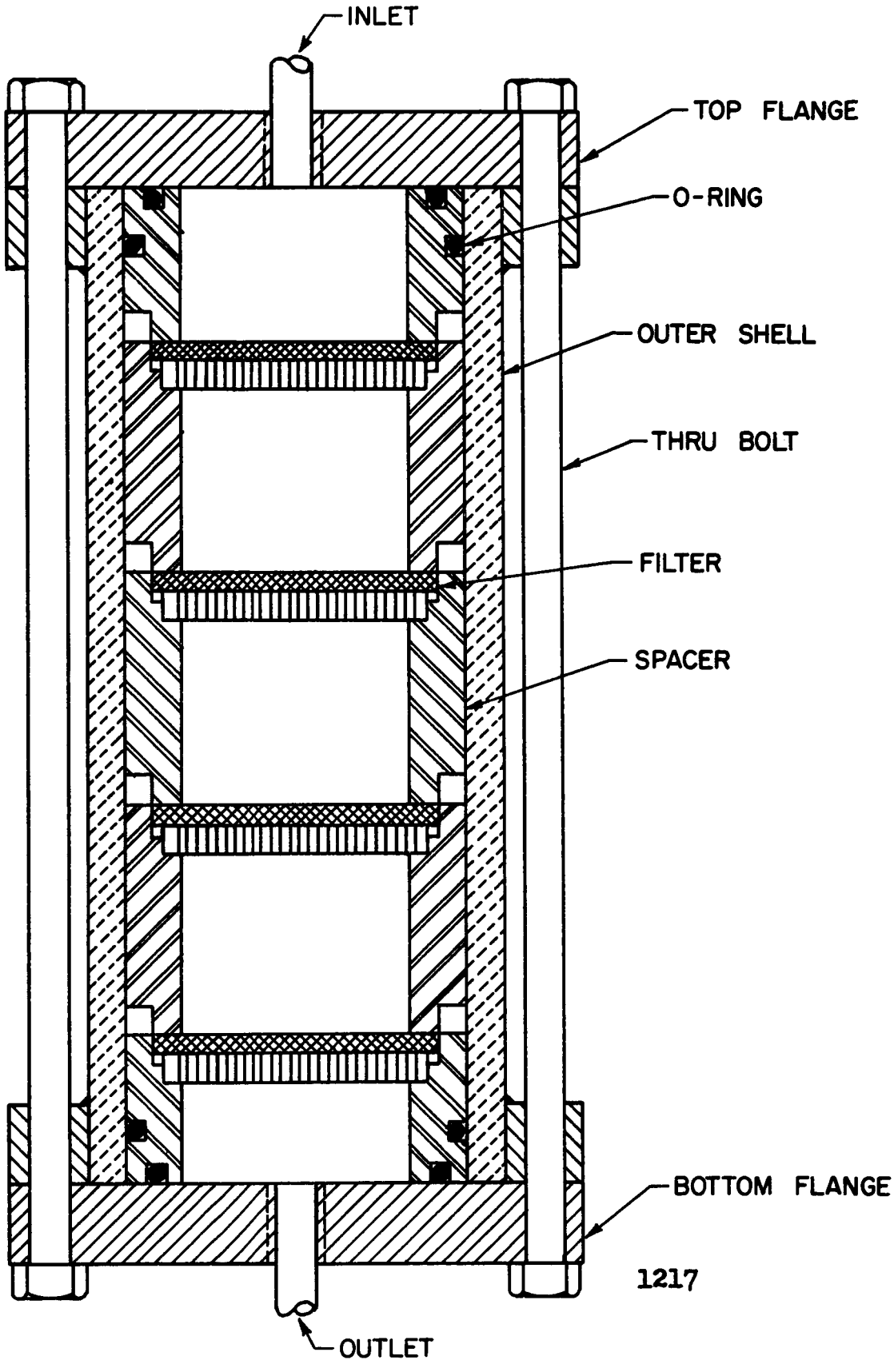

Figure 11. Cross Section of Filtering Rack.

found that the filtering of mercury was much more difficult than that of water for the following reasons:

i) Mercury does not "wet" the filter material as does water, so that the pressure differential necessary to cause it to pass through the small pores is very high (inversely proportional to the pore diameter, assuming the common equilibrium relation between pressure differential and surface tension).

ii) Small debris particles, lighter than mercury, do not easily remain homogenized with the mixture, and very quickly float to the surface. For the vertical down-flow arrangement used the mercury itself may pass through the filters and leave behind the floating debris, containing essentially all the foreign matter. A vertical up-flow arrangement would probably be an improvement in this instance, although harder to handle from the viewpoint of assembly and disassembly without spillage, but that had not yet been tried at the time of the test. However, it is obvious that further development of the filtering technique is imperative, if irradiated specimen tests in mercury are to be employed.

The size of the filters used in the filtering rack were 0.2, 0.8, 10, and 53 microns, with the filters arranged in order of decreasing pore size in the direction of the flow. When only one filter was used, the pore size was 0.2 micron. Although the schedule as shown in Table III was completed, it was not certain that filtration was actually achieved due to the difficulties previously mentioned. In fact, for pore sizes below 0.8 micron, excessive pressure differential is required to force the passage of the mercury, which then apparently passes not through the pores, but through the seal

around the periphery.

The material left on the filters had a relatively homogeneous aspect and its color ran from very dark to almost clear. This debris may have been due to filtration or merely to contact between the rather dirty mercury and the filters. However, as discussed in the next section, the question with respect to this run, becomes academic.

3. Mercury Activity Measurement

It was planned to count the activity on the filters, prepared as described in the last section, using a multiple channel analyzer to determine not only the quantity of radioactive debris as a function of particle size, but also the constituents. However, when this was attempted using the facility of the Michigan Memorial Phoenix Project of this university, no appreciable (i.e., significantly above background) activity was found on any of the filters. A further check with a proportional counter also revealed the almost complete absence of beta activity. Also, no evidence of radioactivity could be found with a Geiger counter outside the loop, although here, of course, the mercury and relatively heavy stainless steel containment structure provides substantial shielding against such activity.

Finally, a 100 cc sample of mercury was withdrawn from the loop and distilled. The residue, and the distilled mercury, were counted to check the possibility of the debris having dissolved into the mercury. Again the results were negative.

A possibility remained that the cavitation damage rate achieved in these tests was an order of magnitude less than anticipated. No direct weight loss measurement was available to refute this possibility, although observation of the specimen surfaces appeared to

indicate that damage had occurred approximately as expected.

Shortly after completion of the run, small sections were removed from the specimens (unfortunately thus obviating the possibility of obtaining a direct weight measurement) to obtain a differential radioactivity characteristic curve for type 302 stainless steel to be available for future tests on this material. This curve is presented as Figure 12.

D. Carbon Steel Specimen Experimental Run

1. General

At the conclusion of the stainless steel test, no real knowledge of the disposition of the radioactive debris (if any) existed. Consequently, it was determined to make a second run with carbon steel for which, according to previous tests with non-irradiated specimens, the damage rate should be considerably greater. The purpose of the carbon steel test was primarily to determine the disposition of the cavitation debris in the loop, and to determine whether subsequent tests of this general type were at all feasible. Hence the procedures used were not nearly so elaborate as for the already described test with stainless steel. Nevertheless, as it occurred, it was possible to obtain certain basic and significant data relative to the cavitation process, as will be described later in this report.

Two annealed 1010 carbon steel specimens were irradiated in the Ford Nuclear Reactor for about 4 months, corresponding to 481 hours of actual reactor operation time. Since the sodium in ordinary glass becomes radioactive, the specimens were encapsulated

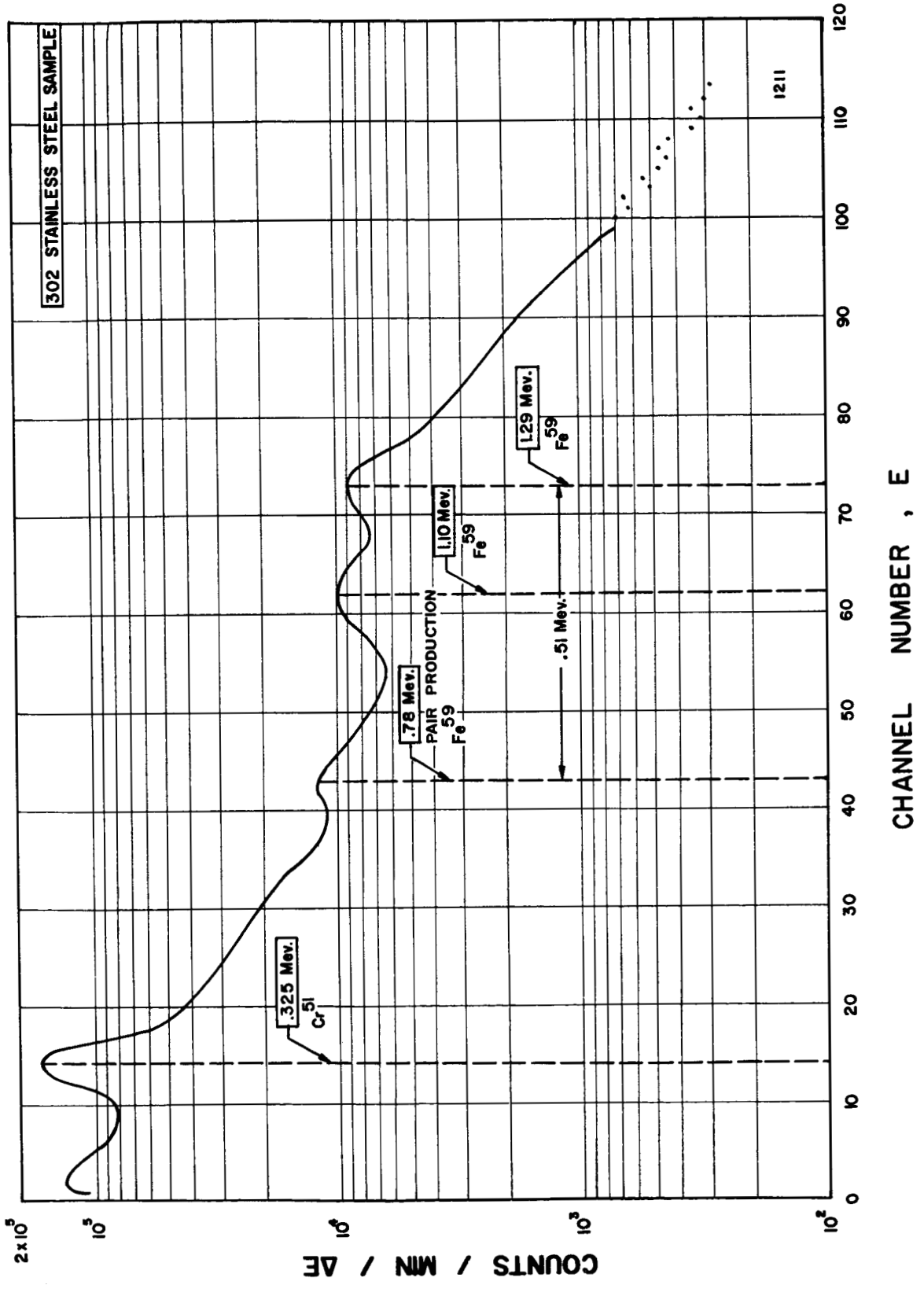

Figure 12. Differential Curve of Stainless Steel Specimen.

in quartz, to prevent corrosion by the water of the reactor pool. This lengthy irradiation time was required, since a dose rate measurement, performed after a month, showed the activity was too low for the purpose. Four days after the irradiation was completed, the dose rate on contact was 2 r/hr, and through the casket shield about 15 mr/hr. Although these values were somewhat less than those which had previously been achieved with the stainless steel specimens (about 5 r/hr on contact, 24 hrs. after completion of irradiation), they were deemed sufficient.

Prior to irradiation, the specimens were examined and photographed under a metallographical microscope to insure that the surfaces were relatively free from imperfections so that cavitation damage, if it occurred, could be distinguished in later examination. Also they were carefully weighed (repeatability of weight measurements is about $\pm$ 0.1 mg.). After the irradiation, and just before insertion in the loop, the specimens were weighed again (See Table IV).

The cavitation damage test was performed for 50 hours continuous duration for the same velocity and cavitation condition previously used with the stainless steel specimens. No mercury samples were taken during the run as the purpose was merely the determination of the distribution of radioactivity, if any, and it did not appear useful at this point, considering the negative results of the previous test, to expend the efforts necessary for the probably fruitless taking and processing of such samples.

At the conclusion of the test, and after removal of the irradiated samples from the vicinity, indications of radioactivity were found at the following locations:

i) In the sump, at approximately the level of the interface separating water and mercury.

ii) At flanges having vertical taps for pipe connections. A sample of 15 cc withdrawn from the loop again showed essentially no radioactivity.

2. Recovery and Counting of Radioactive Debris

Due to the indication of radioactivity from within the loop, it was disassembled in those regions where such indication had been noted, including, of course, the pump sump. It was from this latter location that the major recovery of radioactive debris was made*:

i) Along the inside wall, at the mercury-water interface, there was a deposit of dust-like material of relatively high radioactivity,

ii) Radioactivity was observed in the debris floating on the mercury and under the water.

Samples from these locations were collected on paper and burned. When the ashes were mixed with water for possible filtration, it was found that the filters were immediately clogged. Consequently the ashes were calcined at 1300 ^{o}F., leaving a residue of yellowish powder which could be mixed with water and filtered, assuming that the cavitation debris, being of steel, would be unimpaired by these processes.

Filters of the following openings were used: 53 micron (cloth), 10 micron, 2 micron, and 0.45 micron. The cloth was

---

* Background was about 0.03 mr/hr, reading at the flanges about 0.05 mr/hr, but meter was driven off-scale in the pump sump.

completely plugged by the particles when the filtration was attempted in the filter holder previously described (Figure 10). Hence a larger piece of cloth (3 x 3 inches) was used, and the filtration done without hindrance. Actually, five different pieces of such cloth were required in view of the large amount of debris retained. Four different samples were prepared, corresponding to the four different filter sizes listed above. The last sample, corresponding to the 0.45 micron filter, showed no activity at all, whereas significant activity was observed on the others.

The results obtained from the multiple channel analyzer are plotted in Figure 13. Curve A is the differential curve of the particles retained in the 53 micron filter, curve B corresponds to those contained in the 10 micron filter, and curve C corresponds to the 2 micron filter. All three spectra include the background, which is also plotted in the same figure (curve D). It can be seen that the results from the counting of the 2 micron filter are not very significant, because the order of magnitude of the counts is the same as that of the background. However, the counts corresponding to the 53 and 10 micron filters are very significant, being considerably higher than the background.

After the test, one of the carbon steel specimens was dissolved in concentrated hydrochloric acid heated to about 200 ^{o}F. Suitable precautions were taken to avoid the escape of radioactivity[5]. The resultant liquid was diluted with distilled water to a volume of 250 cc. A 5 cc. sample was taken from this, and again diluted to

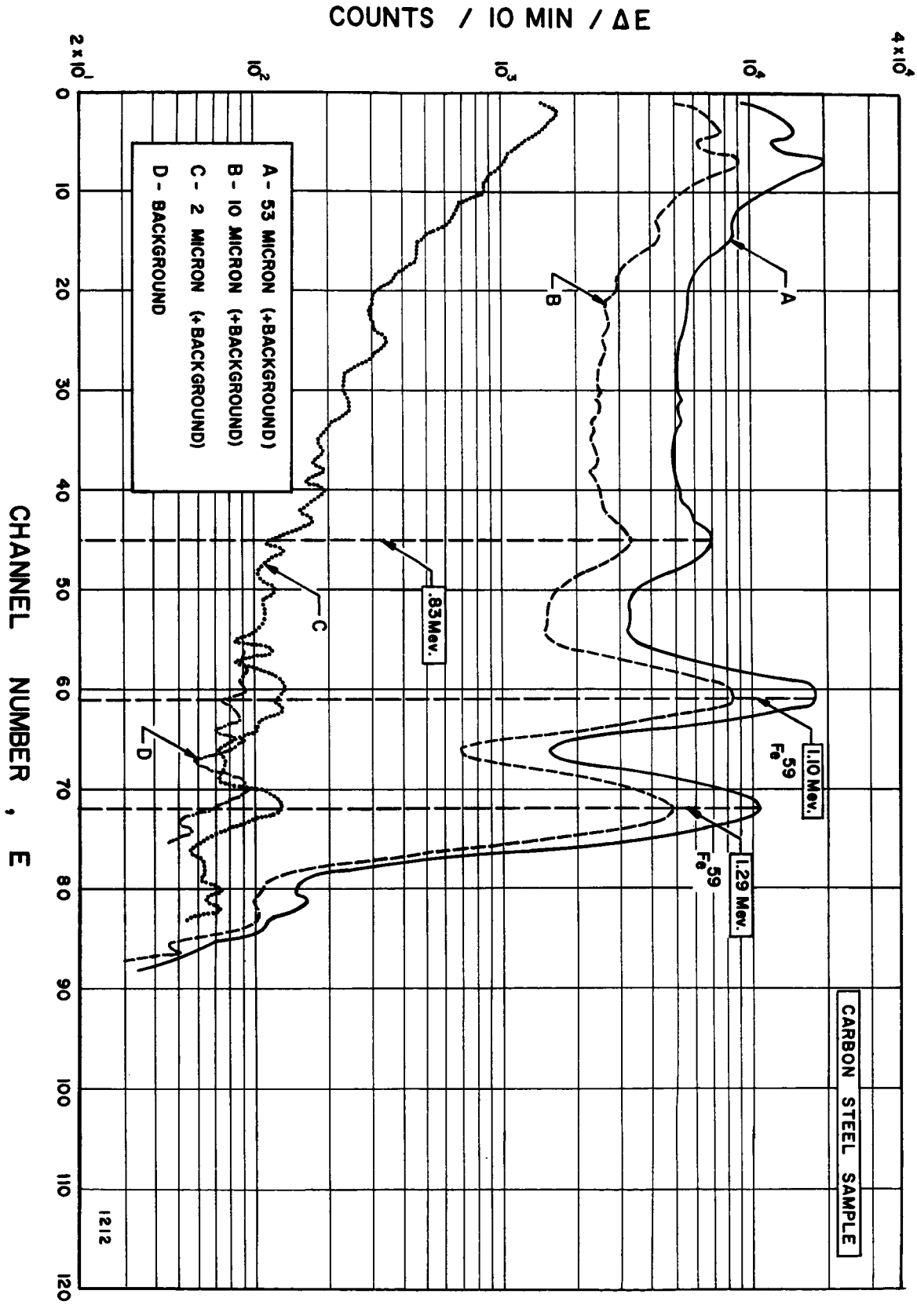

Figure 13. Differential Curves of Debris Retained by the Different Pore Size Filters.

250 cc. Finally, a 2 cc. sample of this solution was counted. The total dilution of the sample was, therefore: (2/250)(5/250)=1/6250.

The differential spectrum obtained from this 2 cc. liquid sample is shown in Figure 14, where also the calibration spectra for Co^{60} and Cs^{137} have been plotted.

The specimens were weighed immediately after the run, and it was noted that they had lost a total of about 5.3 mg. The weights of the specimens at different stages of the experiment are listed in Table IV.

TABLE IV

Weights of Carbon Steel Specimens

(grams)

Date	Specimen 69-1	Specimen 70-1	Remarks
Oct. 2, 1962	3.19750	3.23504	Before irradiation.
Mar. 4, 1963	3.19830	3.23570	After reactor irradiation, but previous to cavitation run, A=20 mr/hr @ 1 ft.
Mar. 27, 1963	3.19491	3.23378	After cavitation run of 50 hours duration.
Weight Loss	0.00339	0.00192	Total weight loss for both specimens: W = 5.31 mg.

III. RESULTS and DISCUSSION of CARBON STEEL TEST

A. General

The data collected this far, and displayed in Figures 13 and 14 is sufficient to calculate the mass of cavitation damage debris recovered from the loop, and make an estimate of the relative size of the particles of metal removed from the specimens during the test.

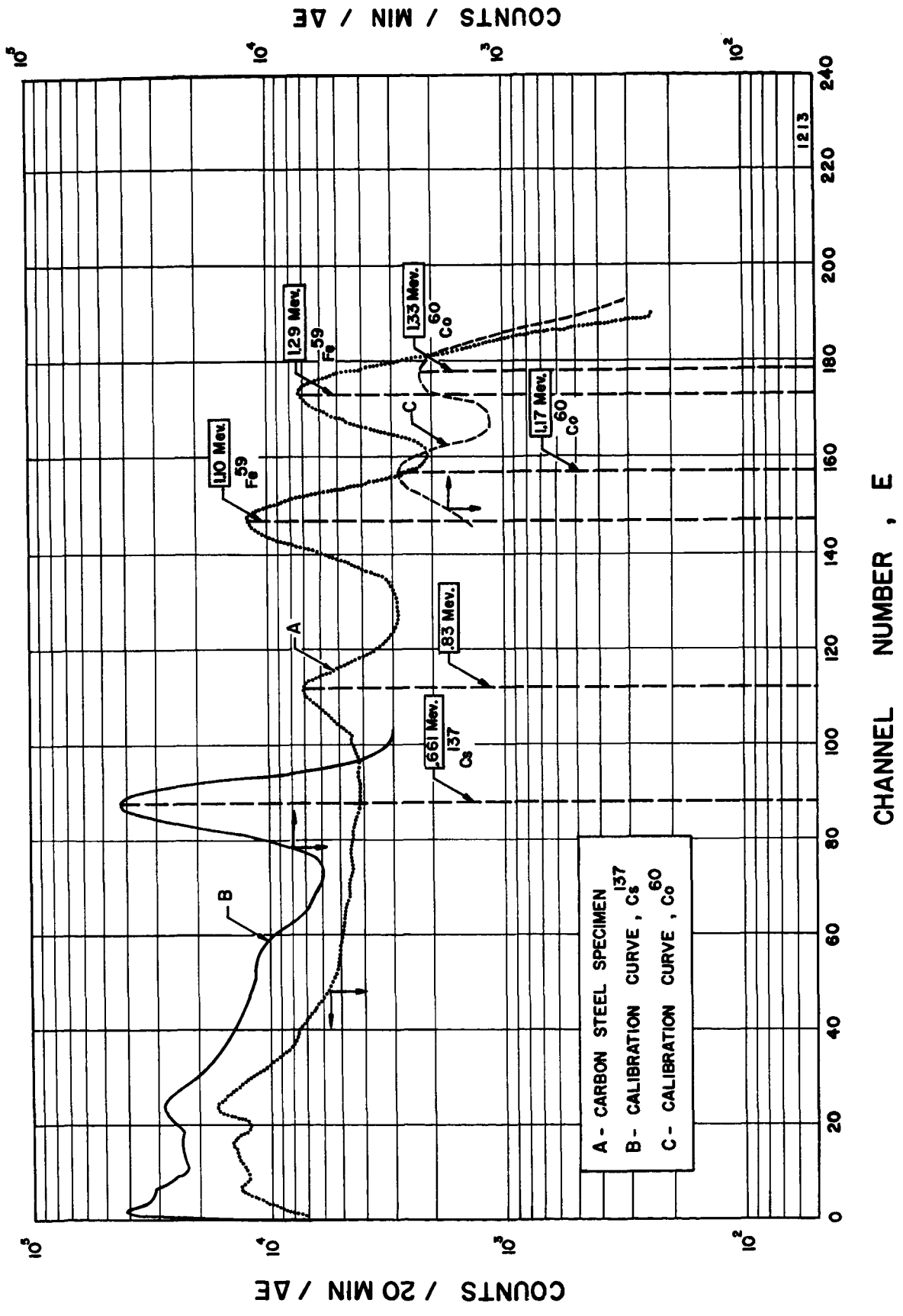

Figure 14. Differential Curve of Carbon Steel Specimen.

Figure 13 shows count-rates measured with a given counting apparatus, a multiple channel analyzer, for gammas emitted from the radioactive debris recovered from the loop within given size ranges, as known from the filter pore size on which the material was trapped. After a suitable energy calibration of the multiple channel analyzer had been performed, as detailed in Section C of the Appendix, it was possible to identify the different photopeaks appearing in the curves, and label them in energy.

Figure 14 shows a differential curve obtained from a standard sample, created by dissolving and diluting one of the original specimens as previously described. The dilution ratio and the original mass of the specimen are known. The sample was counted in the same equipment, and the source-crystal geometry was maintained as close as possible to the arrangement used while counting the differential curves of Figure 13. From the data in Figure 14, a relationship between count-rate and weight of material can be obtained.

Since the material of the radioactive debris and that of the specimen are essentially the same - as discussed later - and were irradiated at the same time, it is possible to compute the mass of material in each size range of the debris, by comparing the corresponding count-rate at a given energy to the count-rate of the standard sample, at the same energy.

It is also possible to establish the similarity, or otherwise, of relative proportions of material constituents between debris and original material, by comparing the relative count-rates at various energy levels, corresponding for example to the gamma ray energies of the different isotopes present in the metal.

In the above comparison it is, of course, necessary to correct the count-rate data to the same chronological time, since there is an unavoidable interval between measurements that can be long compared with isotope half-lives. Knowing the isotopes present and their half-lives, this correction presents no difficulty.

B. Mass of Debris Recovered and Particle Size Distribution

Figures 13 and 14 will be used for the calculation of the mass of material retained in the filters of 53, 10 and 2 micron pore-size. The areas under the higher photopeak of the isotope Fe^{59}, (used because of its better resolution and corresponding to the three differential curves A, B and C, Fig. 13) are calculated, and compared with the same area obtained from Fig. 14. These areas are given in total number of counts per interval of time (in this case, 10 minutes). Since the differential curve given in Figure 14 was obtained on a different date from those on Figure 13, the value of the area under the photopeak of Figure 14 must be corrected back to the day on which the differential curves of Figure 13 were counted. The area under the photopeak can be calculated using the formula*:

$$P = 2.13\ y_m \delta E$$

where: y_m = maximum of the photopeak (counts/unit time/channel)

δE = half-width of photopeak at half-maximum height

---

* See Section D of Appendix.

TABLE V

Mass and Size Distribution of Particles Recovered In The Different Filters

Pore Size		Weight Recovered (mg)	% Recovered of Total Weight Loss	% Retained in Filter	% Passed Through Filter	Size of Particles	
Microns	Mils					Number	Assumed Diameter
53	2.08	.224	4.22	68.95	31.05	6000	53μ
10	0.39	.100	1.89	30.75	.307	14750	30μ
2	.79	.001	0.02	.307	0	18400	6μ
Totals:		.325	6.13%				

The results of the calculations, performed in full detail in Section E of the Appendix, are summarized in Table V. The weight of the debris recovered in each filter is shown, as well as the proportion which this represents of the total measured weight loss of the carbon steel specimens. It was assumed, at this point, that all the radioactive debris had originated from the carbon steel, since there was a considerable lapse of time ($7\frac{1}{2}$ months) between stainless steel and carbon steel experiments, more than sufficient for the radioactivity due to the stainless steel to have decayed to a negligible level. This assumption is strengthened by the fact that the cavitation damage on stainless steel is probably an order of magnitude less than that on carbon steel. Besides, the duration of the stainless steel run was much shorter than for the carbon steel test. Hence, smaller amounts of stainless steel were circulating in the loop.

In addition, Table V shows the number of particles in each size range, assuming them to be spherical and have the density of steel. For the largest category it was assumed that the particle diameter was equal to the specified pore size of the filter on which it was retained.

This assumption is the balance of two factors: (i) some particles smaller than the pore size will be retained because of non-homogeneity of pores, partial blocking by other debris, etc., and (ii) some particles bigger than the pore size will obviously be retained; however, it is doubted, from visual observation of the pits, that many particles much larger than 53 microns (2.08 mils) could have existed. These considerations do not apply for the smaller filter sizes, since the upper cut-off is determined by the next larger filter size. Thus, for the 10 micron filters, the particles could be anywhere between 53 and 10 microns, and an approximate average of 30 microns was assumed for the calculations. Similarly, an average diameter of 6 microns was assumed for the particles retained on the 2 micron filter.

Inspection of Table V reveals that even though most of the mass was retained on the larger filter, the number of particles is much less than that in the next smaller filter size, which is in turn less than that in the smallest filter size. This numerical distribution of particles is consistent with the visual pit count results on any of the non-radioactive specimens which have been tested.

Figure 15 shows the particle size distribution, in terms of percent mass passing through a given filter, as obtained from the carbon steel run in mercury*. Similar data from the previous stainless steel experiment in water[1,2] are also plotted in the same figure for comparison. The curve corresponding to the mercury test is consistently below the one for the water test, indicating that the percentage weight passing through a given filter size is always less for mercury than for water, i.e., the

* It is not especially meaningful to plot the percent retained in each filter versus pore size with only the small number of filters used, since each percentage would include particles of all sizes between the nominal rating of the filter and the next higher size, and thus would give no true indication of the actual weight of the particles of that size.

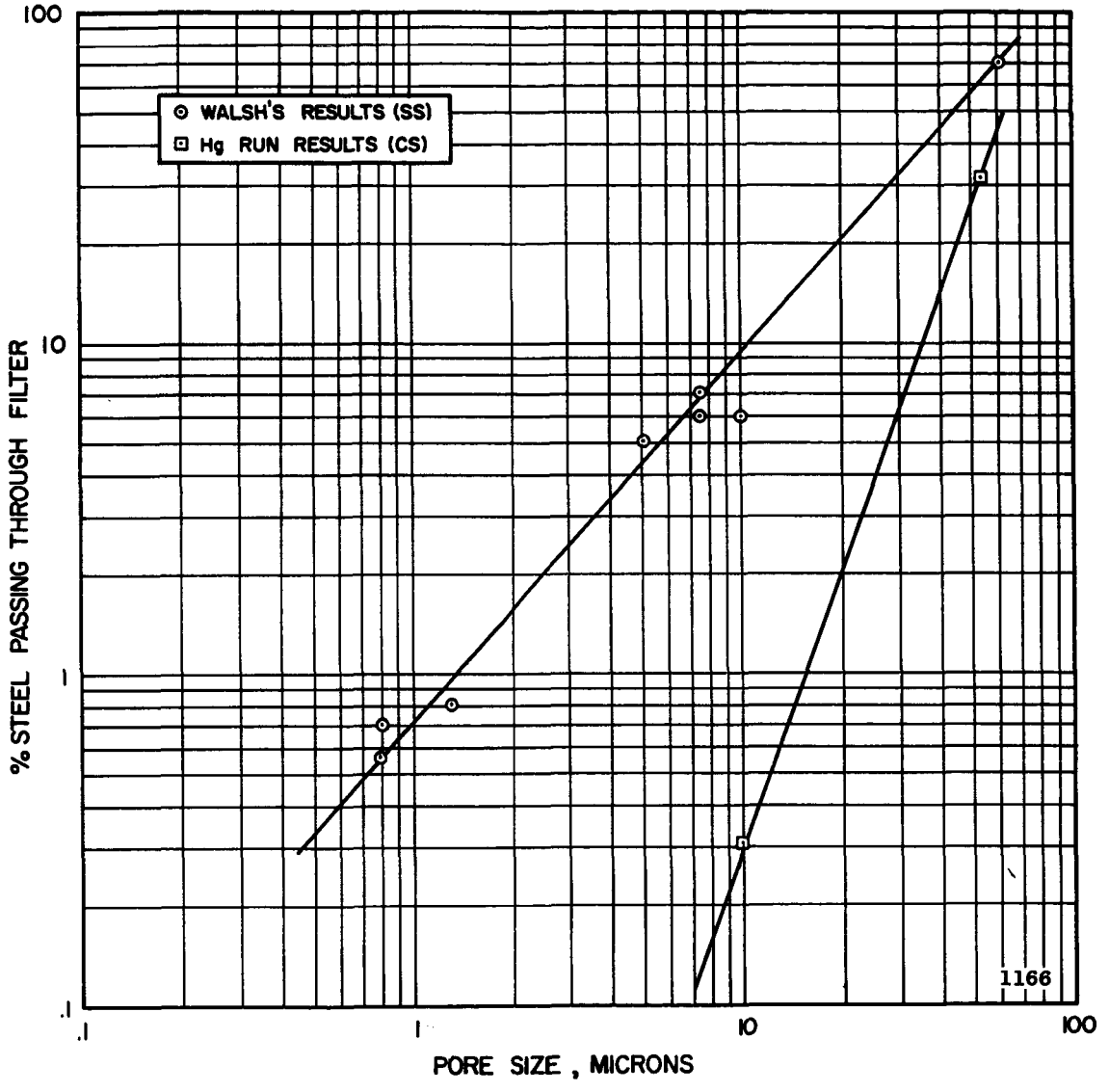

Figure 15. Percent Weight of Steel Passing Through Filters vs. Filter Pore Size.

size of the particles removed by cavitation damage in mercury are relatively larger than in water. However, both curves tend to converge towards the higher pore sizes. Thus, for either fluid most of the debris would pass a filter of 80 microns, i.e., the great majority of the particles are below that size. On the other hand, in the low range, the mercury curve indicates that only a very small percent of debris is of a size less than 6 to 8 microns, while for water, up to about 7% by weight of the particles are below the 8 micron size.

C. Correlation With Visual Pit Counting

Figure 16 shows a composite photomicrograph of the polished face of the carbon steel specimen prior to its irradiation in the Ford Nuclear Reactor. The same specimen, now radioactive, is shown after 50 hours of standard cavitation in Figure 17. Pit tabulation according to size for the regions where the pitting is not yet of the over-lapping type so that individual pits can be distinguished, is presented in Table VI. The size categories tabulated are made to match those of the filters, i.e., greater than 53 microns, 10 to 53 microns and 2 to 10 microns so that a direct comparison can be made. The pit counting was performed on only one of the irradiated specimens.

TABLE VI

Comparison of Number of Pits Observed With Number of Particles of Similar Size in the Debris

Size (dia.)	Counted Pits	Estimate No. of Particles
$D > 53\ \mu$	23	6,000
$53\mu > D > 10\mu$	1,698	14,750
$10\mu > D > 2\mu$	24,415	18,400

As shown in detail in Section E of the Appendix, an estimate of the particle size distribution was made, assuming that the particles were

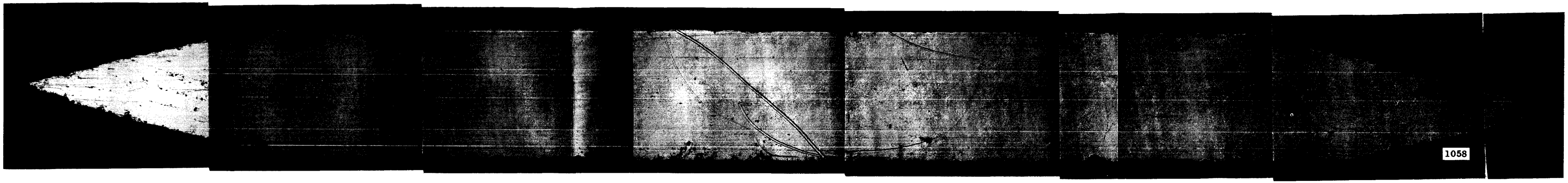

Figure 16. Photomicrograph of Carbon Steel Specimen Prior to Irradiation and Cavitation Damage.

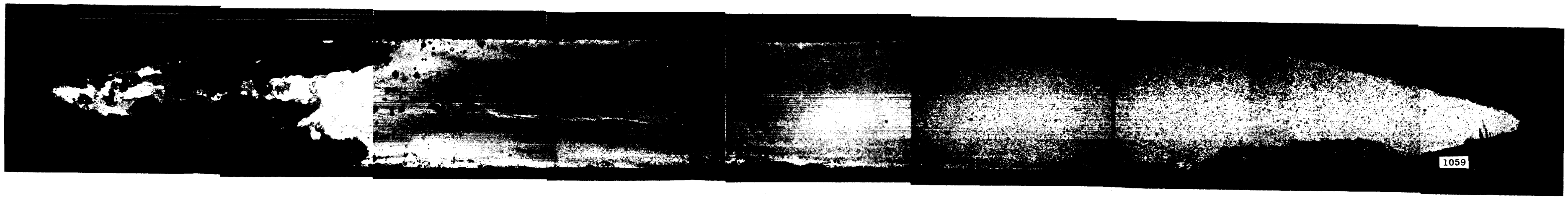

Figure 17. Photomicrograph of Irradiated Carbon Steel Specimen After 50 Hours of Standard Cavitation.

spheres and that the size distribution of the small percentage of debris recovered is the same as in the material that was not recovered. The results of this estimate are also shown in Table VI. Unfortunately, no correlation between these numbers and the number of pits resulting from the actual counting is apparent.

D. Relative Constituents of Debris vs. Original Specimen

The differential curves of Figures 13 and 14 show, within the precision of the available data, that there is no selective attack on the carbon steel, and that the relative constituents of the debris are the same as those of the original specimens, and are not sensitive to particle size. The curves are similar in shape, and show the same peaks. Similar tests with stainless steel, where there may be a real possibility of selective attack by mercury or other liquid metals on the nickel or chromium would be of interest in the future. Unfortunately, as already related, this data was not obtained in the present experiment. However, the fact that the distilled sample and its debris showed no radioactivity does indicate no substantial solution of stainless steel in mercury for this test.

IV. CONCLUSIONS

The following major conclusions may be drawn from the work herein reported:

A. General Feasibility of Method

i) The irradiated tracer technique, while potentially extremely valuable in cavitation-erosion studies with fluids for which disassembly and direct observation are difficult, may require significant development for its implementation, depending upon the particular properties of the fluid-material system. The properties to be considered in this respect

include, for the fluid: wettability, filterability in general, and likelihood of maintenance of relatively homogeneous slurry (which also depends on the flow system configuration); and for the test material, susceptibility to irradiation damage, and existence of suitable isotopes to be used as tracers. As indicated by these tests, and those previously conducted in this laboratory, water-steel is a much more favorable system for this type of test than is mercury-steel. It seems likely that the alkali metals with steel would prove relatively favorable because of the good wetting usually obtained, and the substantial difficulty of direct observation with the accompanying assembly and disassembly.

ii) The irradiated tracer technique, in a centrifugal-pump-driven tunnel facility as used herein, is not suitable for direct weight loss determinations in general because of the likelihood of separation in strong vortices as in the pump, various pipe bends, etc.

iii) The irradiated tracer technique is a useful, and perhaps the only feasible, method available for the determination of debris particle-size distribution and relative constituents, as compared with the undamaged material.

B. Particular Experimental Results

i) The centrifugal pump has a strong separating influence on particles of low density relative to the fluid, trapping them in the pump sump. This implies the existence of a strong degassing effect, and also the probable elimination from the mercury of immiscible fluids as water during pump operation.

ii) A particle-size distribution for cavitation damage on type 1010 carbon steel* by mercury was obtained, and compared with a

* In an annealed condition.

similar measurement previously obtained for type 302 stainless steel* in water[1,2]. The indicated maximum particle size was about the same in both cases (~3 mils). However, the mercury particle size range was not as great, showing fewer particles of minimum size. It was determined that the size distribution is not consistent with the microscopic examination of the damaged surfaces.

iii) Evidence that selective attack did not occur on the carbon steel was obtained by comparison of the differential curves resulting by the debris and the original specimen. It was also verified that the constituents of the debris did not vary according to size range.

---

* In annealed condition.

BIBLIOGRAPHY

1. Walsh, W. J., "Cavitation Damage Measurements With Radioisotopes", Internal Report No. 4, ORA Project 03424, The University of Michigan, February 1961.

2. Walsh, W. J., and Hammitt, F. G., "Cavitation and Erosion Damage and Damage Particle-Size Measurements with Radioisotopes", Nucl. Sci. and Engr., 14, No. 3, November 1962.

3. Hammitt, F. G., et al., "Cavitation Damage Tests With Water in a Cavitating Venturi", ORA Report 03424-4-T, The University of Michigan, April 1962.

4. Hammitt, F. G., et al., "Cavitation Damage in Mercury and Water in a Cavitating Venturi and Other Components", ORA Report 03424-9-T, The University of Michigan, September 1963.

5. Nieto, J. M., "Cavitation Damage Measurements by Radiotracer Analysis", Master's Thesis, Department of Nuclear Engineering, The University of Michigan, May 1963.

6. Smith, W., et al., "On The Production of Radioactive Isotopes by Neutron Irradiation", Internal Report No. 16, ORA Project 03424, The University of Michigan, September 1962.

7. Harris, D. R., et al., "Radiation Damage in Iron and Steel", Nuclear Power, 47, 97-9, 1960.

8. Thomas, D. E., "Radiation Damage in Ferrous Metals", J. Metals II, 523-27, 1959.

9. Radiological Health Handbook, U. S. Department of Health, Education, and Welfare, PB 121784, 1960.

10. Harvey, J. A., and Hughes, D. J., "Neutron Cross Sections", BNL-325, 1958.

11. Way, K., et al., "Nuclear Level Schemes", TID-5300, 1955.

12. Nuclear Data Sheets, National Academy of Sciences, National Research Council, 59-2-24.

13. Marinelli, L. D., et al., "Dosage Determination With Radioactive Isotopes", American Journal of Roentgenology, 59, 260-81, 1948.

14. Handbook of Chemistry and Physics, 42nd Edition, Chemical Rubber Publishing Co., Cleveland, Ohio, 1960-61.

APPENDIX

A. Estimate of Stainless Steel Specimen Activity

The first problem to be solved is the estimation of the activity per gram of the irradiated specimen, assuming a neutron thermal flux of 5×10^{12} neutrons/cm^2/sec. which corresponds to the nominal operating conditions, i.e., one megawatt, of the Ford Nuclear Reactor.

Let R be the no. of atoms formed per sec. by absorption of neutrons per unit mass of sample. Then

$$R = \frac{\text{Reaction rate}}{V\rho} \qquad (1)$$

where V = volume of sample (cm^3), and ρ its density (gm/cm^3), and $V\rho$ = mass of the sample, gms.

The reaction rate for absorption processes is calculated as follows:

$$\text{Reaction rate} = V \int_0^{E_T} N\rho\,\sigma_a(E)\,\phi(E)\,dE \qquad (2)$$

where:

N = number of atoms of the isotope in consideration per gram of sample.

ρ = density of sample in grams per cm^3

$\sigma_a(E)$ = absorption cross section which depends on the energy of the neutron.

$\phi(E)$ = neutron flux in neutrons/cm^2/sec /unit energy interval.

E_T = maximum value of neutron energy.

Therefore:

$$\text{Reaction rate} = V\rho N \int_0^{E_T} \sigma_a(E)\,\phi(E)\,dE \qquad (3)$$

or:

$$\text{Reaction rate} = V\rho N\,\phi_T\,\bar{\sigma}_a = V\rho N \frac{\sigma_a}{1.128}\,\phi_T \qquad (4)$$

where:

ϕ_T = thermal flux = $\int_0^{E_T} \phi(E)\,dE$

$\bar{\sigma}_a$ = average absorption cross section for thermal flux.

σ_a = thermal absorption cross section (listed in barns in column 6, Table II).

The factor 1.128 appears since:

$$\bar{\sigma}_a = \frac{\sqrt{\pi}}{2}\sigma_a = \frac{\sigma_a}{1.128}$$

when a Maxwell-Boltzmann distribution of the thermal neutron energies is assumed. Thus, the value of R is finally:

$$R = \frac{N \sigma_a \phi_T}{1.128} \qquad (5)$$

Since the radioactive atoms formed after the irradiation of the sample start to decay immediately after their formation, the net change in the number of radioactive atoms per unit time is expressed for each isotope:

$$\frac{dn(t)}{dt} = R - \lambda n(t) \qquad (6)$$

where $n(t)$ is the number of radioactive atoms per gram of sample present at time t, and λ the disintegration constant. Since the number of radioactive atoms present at time $t = 0$ is zero, the solution to eq. (6) is:

$$n(t) = \frac{R}{\lambda}(1-e^{-\lambda t}) \qquad (7)$$

Thus, the activity in disintegrations per second per gram of sample at time t will be given by:

$$A(t) = R\,(1 - e^{-\lambda t}) \qquad (8)$$

If the specimen is to be irradiated for a period of several days, formula (8) cannot be correctly applied, since the reactor does not operate on a continuous schedule. For this reason the activity per gram of sample has been investigated under the assumption that the reactor is operating for a continuous period of 8 hours a day and then shut down for the next 16 hours. Using the results given in Reference 6, the activity per gram of sample due to an isotope with a decay constant λ, or a half-life $T_{\frac{1}{2}} = 0.693/\lambda$, after n days of irradiation

is given by:

$$A_{e_n} = A_\infty K \left[1-e^{-nc}\right] \qquad (9)$$

where:

A_∞ = saturation activity = $R \frac{\text{disintegrations/sec.}}{\text{gram}}$

$K = \frac{1-e^{-c/3}}{1-e^{-c}}$

$C = 24\lambda$, where λ is in hr^{-1}

The calculations of the activities for the five isotopes of interest are summarized in Table I-A. In column one, the isotopes are listed. In column two, the saturation activities are computed using the formula:

$$A_\infty = \frac{N\sigma_a\phi_T}{1.128 \times 10^{12}}$$

obtained from (5) when the thermal absorption cross sections are expressed in barns. The thermal flux, ϕ_T, is assumed to be 5×10^{12} $\frac{\text{neutrons}}{cm^2\ sec}$, corresponding to 1 MW power level of the FNR. The values of N and σ_a are taken respectively from columns five and six of Table II in the text.

In column three, the disintegration constants are given in inverse hours. In columns four and five, the values of K and c are given as calculated in Reference 6. Using formula (9) for n = 20, the values of A_{e_n} are computed and the results are recorded in column six of Table I-A.

At the moment when the specimens are removed from the reactor, the activity of each isotope is given in mc/gm of sample by the formula:

$$S = \frac{A_{e_n}}{3.7 \times 10^7} \qquad (10)$$

The corresponding calculated values are given in column seven of Table I-A. The total activity of the two samples used in the experiment due to each isotope will be:

TABLE I-A

Estimate Activities of the More Important Isotopes Contained in the Stainless Steel Specimens

Line*	Isotope	A_∞ Dis/sec/g	λ	K	c	A_{e_n} (n = 20)	S_o (mc/gm)	S_{o_T} (mc)
4	Fe-59	1.025×10^{8}	6.41×10^{-4}	0.335	1.538×10^{-2}	9.1×10^{6}	0.242	1.55
5	Mn-56	8.28×10^{9}	0.27	0.885	6.45	7.33×10^{9}	1.98×10^{2}	1.268×10^{3}
9	Cr-51	6.44×10^{9}	1.035×10^{-3}	0.338	2.482×10^{-2}	8.53×10^{8}	23.04	1.475×10^{2}
17	Ni-65	8.60×10^{7}	0.27	0.885	6.45	7.61×10^{7}	2.055	13.16
38	Co-60	2.72×10^{8}	1.5×10^{-5}	0.333	3.6×10^{-4}	6.53×10^{5}	1.763×10^{-2}	0.113
	(1)	(2)	(3)	(4)	(5)	(6)	(7)	(8)

* Correspond with the lines in Table II in the text.

$$S_{T_o} = \frac{A_{e_n} \times 3.2 \times 2}{3.7 \times 10^7} \quad mc = S_o \times 6.4 \quad mc \qquad (11)$$

assuming an average weight of 3.2 grams per specimen.

Now we are interested in the dose rate, which is given by the formula:

$$D = 10^3 \quad \frac{R_o \, S_{T_o}}{r^2} \quad \frac{r}{hr} \qquad (12)$$

where: S_{T_o} = source strength, curies

r = distance from source, centimeters

$R_o = R_o(E_\gamma)$ = specific radiation flux, r/hr/mc at 1 cm.

The values of R_o are given by Marinelli[13]. When more than one gamma ray is ejected per disintegration, the total R_o is given by the expression:

$$R_o = \sum_i R_o(E_i) n_i \qquad (13)$$

where n_i is the number of gammas per disintegration with energy E_i, and $R_o(E_i)$ is the specific radiation flux corresponding to energy E_i.

Figures 6, 7, and 8 show the decay schemes of the isotopes of interest as used for the calculations of R_o given in column five of Table II-A.

Using formula (12), dose rates in r/hr were calculated at a distance of 100 cm at the time of removal of the samples from the neutron flux (t = 0). The dose rates were also computed at distances 100 cm and 1 cm for t = 24 hours, corresponding to the time when actual measurements of the activity of the specimens were performed. The results are listed in Table III-A. It can be seen that the measured dose rate was much less than the estimated value resulting from this calculation.

TABLE II-A

Values of the Specific Radiation Flux R_o For the Isotopes of Interest

Line	$T_{1/2}$	Isotope	S_{o_T}(mc)	Gamma-energy Mev (o/o)*	R_o $\frac{r}{hr\text{-}mc}$ @ 1 cm
4	45.1d	Fe-59	1.55	0.191 (3.1%) 1.098 (57%) 1.289 (43%)	6.55
5	2.59h	Mn-56	1,268	0.845 (100%) 1.76 (30%) 2.17 (20%)	9.55
9	27.9d	Cr-51	147.5	0.325 (9%)	0.171
17	2.564h.	Ni-65	13.16	1.49 (18.1%) 1.12 (12.9%) 0.37 (4.9%)	2.38
38	5.24y	Co-60	0.113	1.172 (100%) 1.332 (100%)	13.5
	(1)	(2)	(3)	(4)	(5)

* Percentages indicate the number of gamma rays of that energy ejected per 100 disintegrations.

TABLE III-A

Estimated Dose Rates For Stainless Steel Specimens

Isotope	$T_{1/2}$	Dose Rate D (r/hr)		
		t = 0 d = 100 cm	t = 24 hr d = 100 cm	t = 24 hr d = 1 cm
Fe-59	45.1d	1.016×10^{-3}	1.01×10^{-3}	10.1
Mn-56	2.59h	1.21	1.875×10^{-3}	18.75
Cr-51	27.9d	2.52×10^{-3}	2.46×10^{-3}	24.6
Mi-65	2.564h	3.13×10^{-3}	4.85×10^{-6}	0.0485
Co-60	5.24y	1.525×10^{-4}	1.525×10^{-4}	1.525
TOTAL DOSE		1.2168	0.0045	45.0235

B. Estimate of Activity of Mercury Samples

The total weight of mercury in the loop is about 671 lbs., which corresponds to a volume of:

$$\frac{671 \text{ lbs.}}{13.534 \text{ gr/cm}^3 \times .0022 \text{ lbs./gr.}} = 22{,}550 \text{ cm}^3$$

The weight of a specimen is about 3.2 grams, and based on previous tests, it was estimated that about 1.20 mg. per specimen would be removed during the experiment. Hence, the dose rate from a 50 cm^3 mercury sample (selected as a convenient size) is given by the expression:

$$\frac{2 \times 1.2 \times 50}{22{,}550} \; D \qquad \frac{r}{hr}$$

where D is the total dose rate per mg. of specimen after completion of the run. As given by Table III-A, the theoretical total dose rate of the two specimens, at 1 cm, and 24 hours after the end of the irradiation,

was: 45.0235 r/hr. After the completion of the run, the dose rate will be substantially due only to the isotopes Fe^{59}, Cr^{51}, and Co^{60}, since Mn^{56} and Ni^{65} have relatively short half-lives. Thus, the total dose of the two specimens would be 36.2 r/hr (See Table III-A), if it is assumed that the activity of Fe^{59} and Cr^{61} is not appreciably reduced during the period of time between the end of the irradiation of the specimens and the completion of the run. The dose rate of 36.2 r/hr corresponds to a weight of 2 x 3.2 = 6.4 grams, so that the factor D in the formula on the previous page will be equal to 36.2 r/hr divided by 6.4 gm. Then, the dose rate of a 50 cm^3 mercury sample will be:

$$\frac{2.40 \times 50}{22,550} \times \frac{36.2}{6.4 \times 10^{-3}} = 0.0302 \ \frac{mr}{hr} \ @ \ 1 \text{ cm}$$

Assuming that there were only Fe-59, (as had been assumed in the previous work[1,2]) the activity of the two specimens of stainless steel would be 1.55 mc (vs. about 149 mc considering also Cr^{51} and Co^{60}) corresponding to a weight of 6.4 grs. The activity of a sample of 50 cc taken after completion of the run would be:

$$A_s = \frac{1.55 \times 2.4 \times 50 \times 10^{-3}}{6.4 \times 22500} = 1.29 \times 10^{-6} \text{ mc/sample}$$

If this sample is counted, for instance, in a counter with 50% efficiency and 2π geometry, the area under the 1.10 Mev Fe-59 peak will be:

$$C_s = 1.29 \times 10^{-6} \times 3.7 \times 10^{7} \times \frac{2\pi}{4\pi} \times \frac{50}{100} \times \frac{57}{100} \text{ counts/min.}$$

or,

$$C_s = 410 \text{ counts/min./sample.}$$

The factor 57/100 has been introduced since Fe-59 emits the 1.10 Mev gamma ray in 57% of the disintegrations. Since the background is of the order of 50 counts/min., such a count rate would be detectable.

To improve the statistics the counting time can be increased. A 20-minute counting time would give a standard deviation of 89.4 counts/min. equivalent to 1.11% (vs. about 5% for a 1-minute count).

C. Calibration of the Multiple Channel Analyzer

The calibration in energy of the MCA was accomplished by obtaining the differential curves of Co^{60}, Cs^{137} and Na^{22}. These curves are shown in Figure 1-A, where the energies of the different photopeaks have been indicated. Using this information, a plot of gamma ray energy versus channel number was obtained, (Figure 2-A). As expected, the relationship between these two quantities is linear.

On the basis of the calibration curve shown in Figure 2-A, then, the different photopeaks appearing on the differential curves plotted in Figures 11, 12, and 13 were labeled in energy, and subsequently identified.

D. Evaluation of the Area Under the Photopeak

In the usual representation of differential curves, Figure 3-A, the abscissas represent the channel number E (proportional to pulse height), while the ordinates represent the count rate corresponding to each interval ΔE. The channel number E is also proportional to the gamma ray energy E_γ.

The total number of counts per unit time, produced by gamma rays of energy E_γ will be given thus by the area under the photopeak:

$$P = \int_{-\infty}^{\infty} y(E)dE \qquad (1)$$

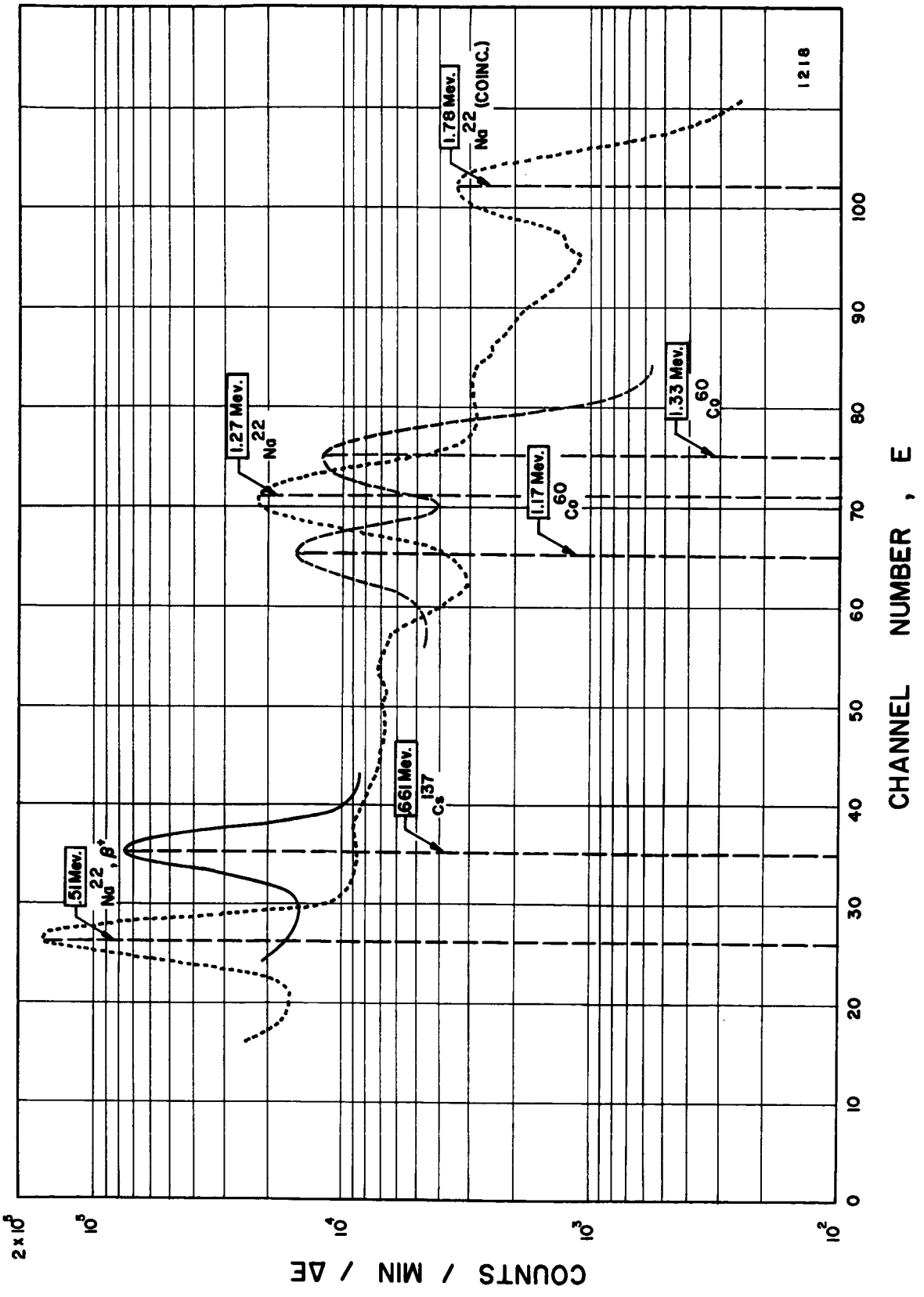

Figure 1A. Differential Curves of Co^{60}, Cs^{137} and Na^{22}.

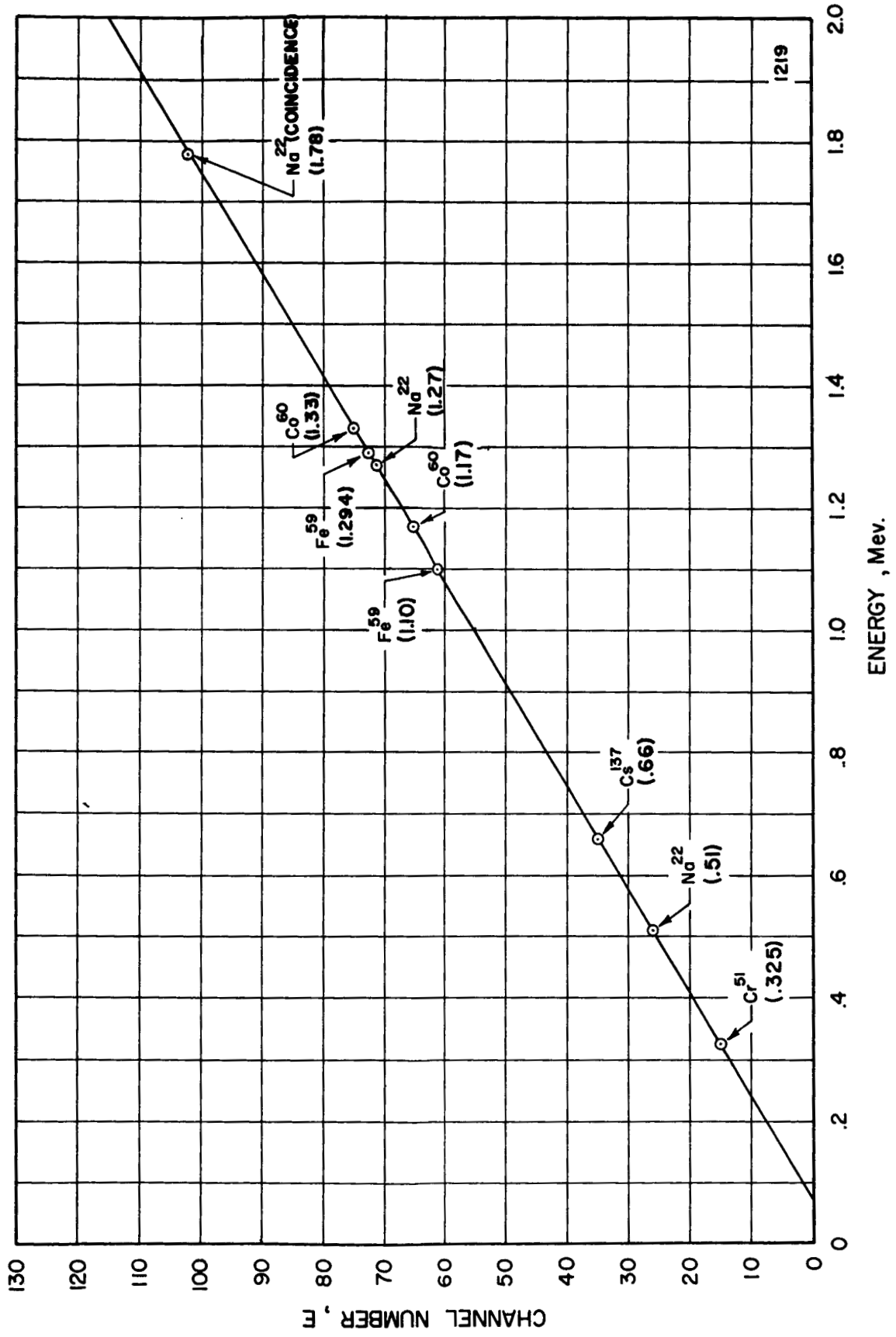

Figure 2A. Calibration Curve for MCA: Channel Number versus Gamma-ray Energy.

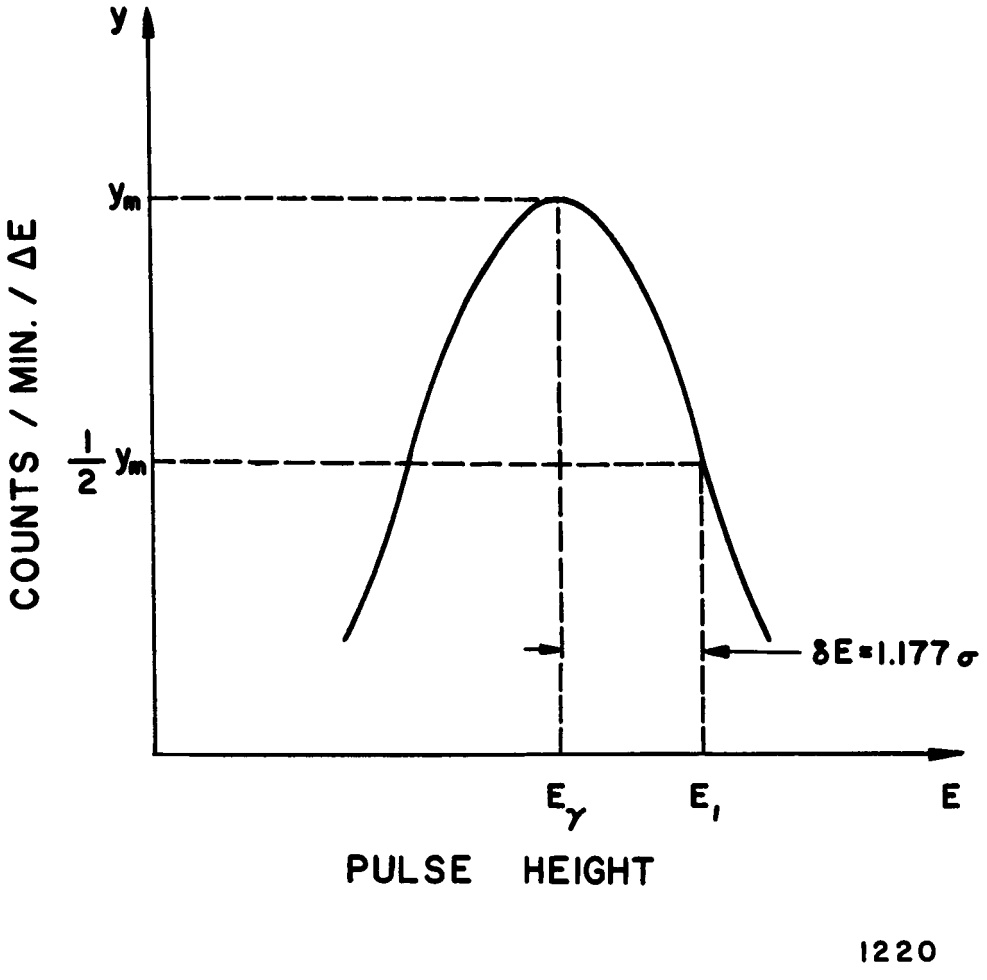

Figure 3.A Photopeak for Gaussian Distribution About Gamma-Ray Energy.

If a truly Gaussian distribution about E_γ is assumed, then:

$$y(E) = y_m \exp\left[-\frac{(E - E_\gamma)^2}{2\sigma^2}\right] \qquad (2)$$

and by substitution in equation (1):

$$P = y_m \int_{-\infty}^{\infty} \exp\left[-\frac{(E - E_\gamma)^2}{2\sigma^2}\right] dE = \sqrt{2\pi}\, y_m \sigma \qquad (3)$$

By making $y = \frac{y_m}{2}$ in equation (2), one obtains:

$$\frac{1}{2} = \exp\left[-\frac{(E_1 - E_\gamma)^2}{2\sigma^2}\right]$$

and from here:

$$\sigma = \frac{E_1 - E_\gamma}{\sqrt{2 \ln 2}} = \frac{\delta E}{1.177}$$

Finally, by substitution into (3):

$$P = 2.13\, y_m\, \delta E \qquad (4)$$

Here, P is expressed in counts per unit time. The quantity $2\delta E$ is the width of the photopeak at half-height. Both δE and y_m can be obtained directly from the differential curves under consideration.

E. Mass of Debris Recovered and Particle Size Distribution

1. Debris Recovered

During the experiment with the carbon steel specimens, the following differential curves were obtained:

i) Figure 13 is from a calibrated sample, prepared as described in the text. This establishes a relationship between activity and weight of material.

ii) Figure 12 is from the debris retained in the different pore size filters.

The Multiple Channel Analyzer was the same, and the geometry,

i.e., the arrangement of the sample with respect to the crystal, was maintained as constant as feasible. Consequently, by comparing the areas under the photopeaks of a particular isotope, it is possible to ascertain the relative activities of the debris of that isotope retained by the different filters, and by using the mass to activity relationship given by (a), to determine the actual weight of those debris.

The calculations are carried out for the 1.10 Mev photopeak of Fe^{59}, selected because of its better resolution.

In Figure 4-A, the 1.10 Mev photopeak of Fe^{59} corresponding to the calibrated sample is plotted again in a linear scale. The number of counts have been corrected for background using an average of 52 counts per 10 minutes, and the ordinates of the curve are given in net counts per ten minutes per ΔE. As easily obtained from Figure 4-A, the value $2\delta E$ is equal to 12.2 channels, while y_m = 6037. Using formula (4), the area under the photopeak is then:

$$P = 2.13 \times 6037 \times \frac{12.2}{2}$$

or:

$$P = 7.84 \times 10^4 \frac{\text{counts}}{10 \text{ min.}}$$

This photopeak was obtained on May 15, 1963, at 5 p.m., while the rest of the differential curves were counted on March 12, 1963, at 4 p.m., i.e., 65.04 days earlier. Correcting for the decay of the sample, one has:

$$P_o = Pe^{\lambda t}$$

where:

$$\lambda = 6.41 \times 10^{-4} \text{ hr}^{-1}, \text{ for } Fe^{59}$$

and:

$$t = 65.04 \times 24 \text{ hrs.}$$

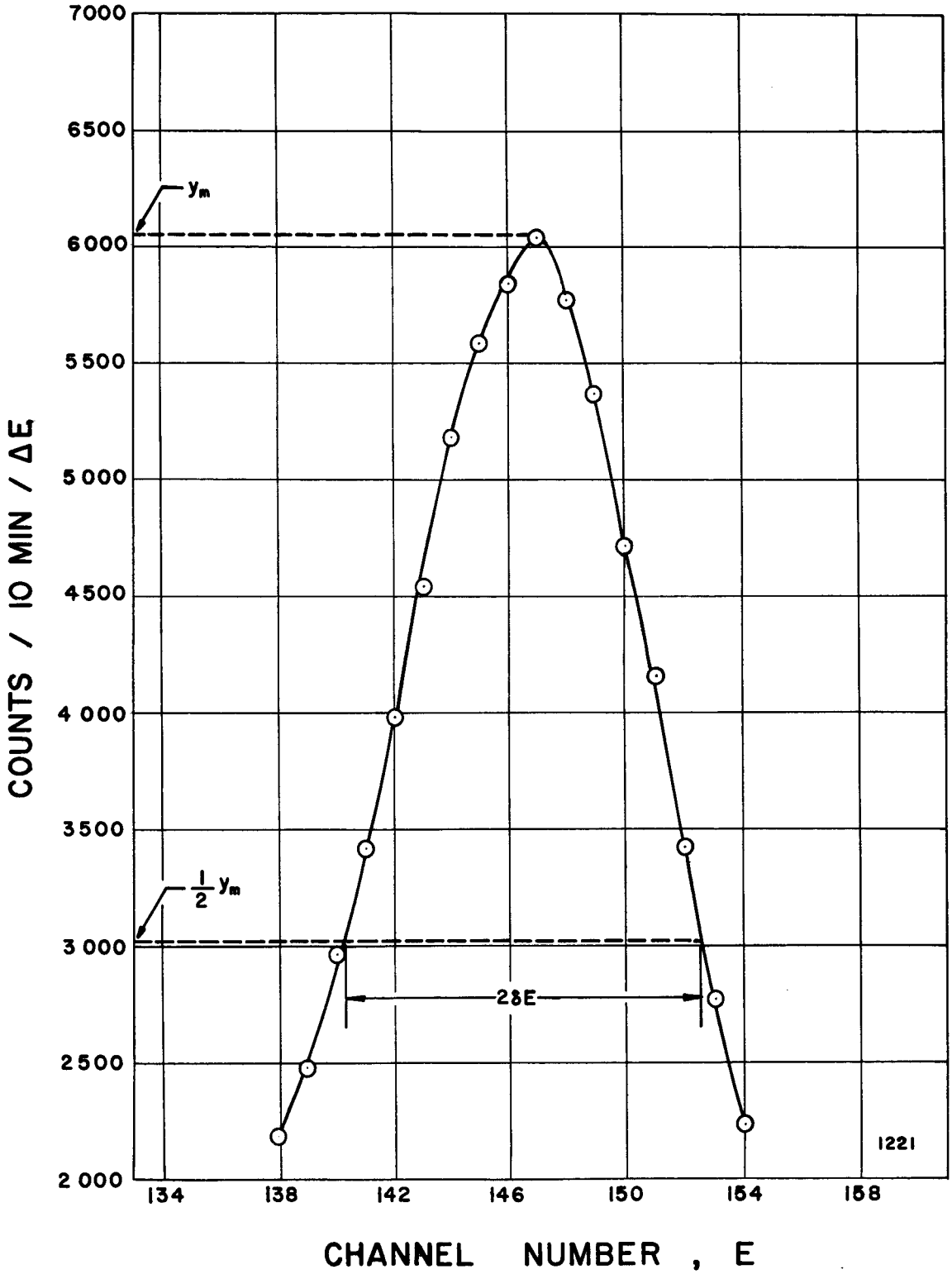

Figure 4A. 1.10 Mev Photopeak of Fe^{59} in Calibrated Sample.

Thus:

$$P_o = 7.84 \times 10^4 \exp (6.41 \times 10^{-4} \times 65.04 \times 24)$$

or:

$$P_9 = 2.14 \times 10^5 \frac{\text{counts}}{10 \text{ min.}}$$

This value of P_o corresponds to a weight:

$$W_o = \frac{W}{6250}$$

where W, the weight of the specimen, is given by Table IV as:

$$W = 3.23378 \text{ grams}$$

Hence, the conversion factor can be written:

$$C = \frac{W_o}{P_o} = \frac{3233.78/6250}{2.14 \times 10^5} = 2.415 \times 10^{-6} \quad \frac{\text{mg}}{\text{counts/10 min.}}$$

The 1.10 Mev photopeak of Fe^{59} for the debris retained on the 53 micron filter is shown in Figure 5-A. From this figure, the following values are obtained: $2\delta E = 4.9$ channels, and $y_m =$ 17,751 counts/10 min./channel. The area under the photpeak is therefore:

$$P_{53\mu} = 2.13 \times 17{,}751 \times \frac{4.9}{2} = 9.26 \times 10^4 \frac{\text{counts}}{10 \text{ min.}}$$

and the corresponding weight of the debris, in milligrams, is:

$$W_{53\mu} = P_{53\mu} \times C = 9.26 \times 10^4 \times 2.415 \times 10^{-6}$$

or:

$$W_{53\mu} = 0.224 \text{ mg}$$

Since the total weight loss for both specimens was 5.31 mg (See Table IV), these 0.224 mg correspond to a percentage of:

$$\frac{0.224}{5.31} \times 100 = 4.22\%$$

The photopeak corresponding to the debris retained on the 10 micron filter is shown in Figure 6-A. From here: $2\delta E = 4.70$ and

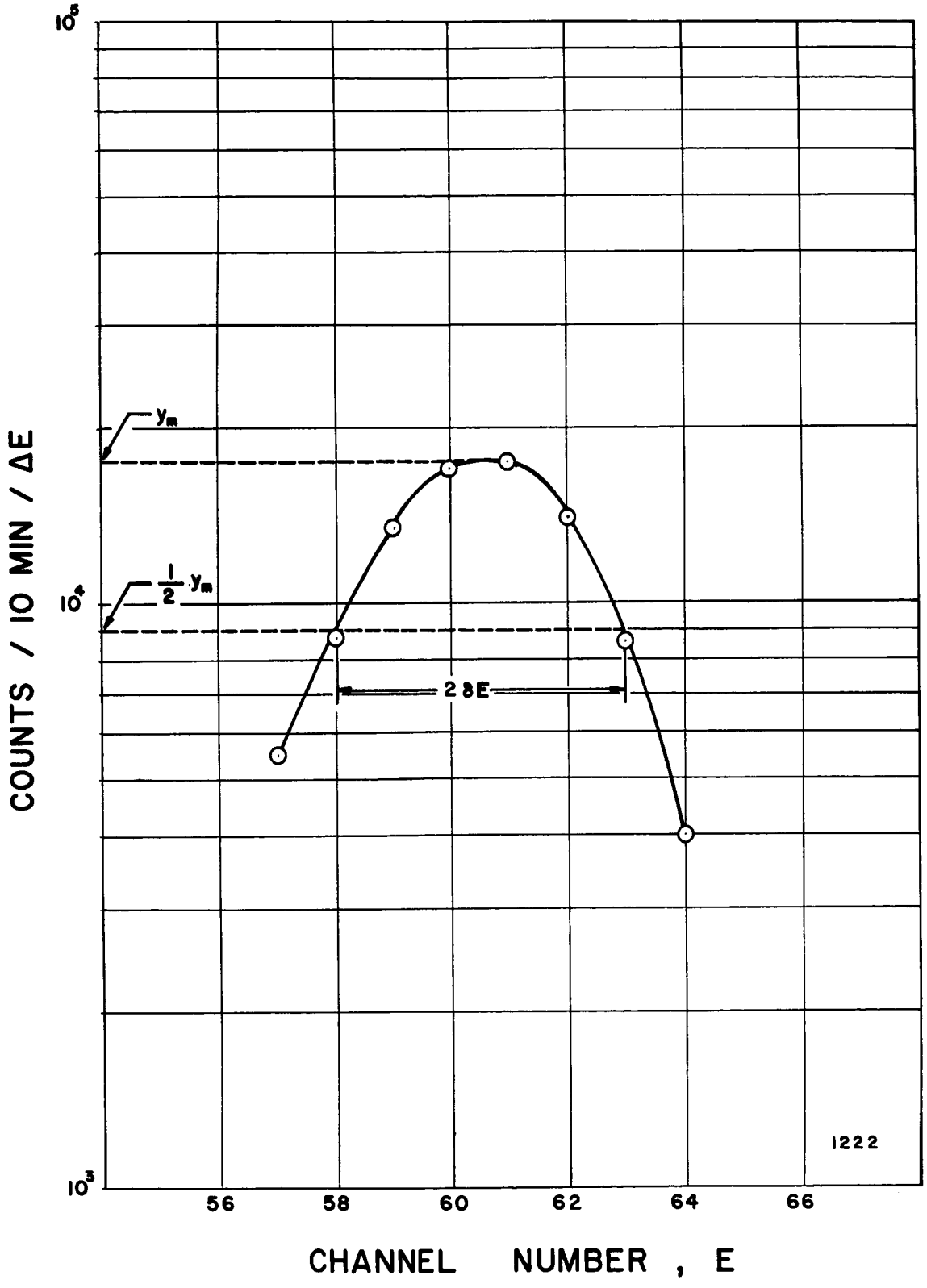

Figure 5A. 1.10 Mev Photopeak of Fe^{59} Retained on 53 Micron Filter.

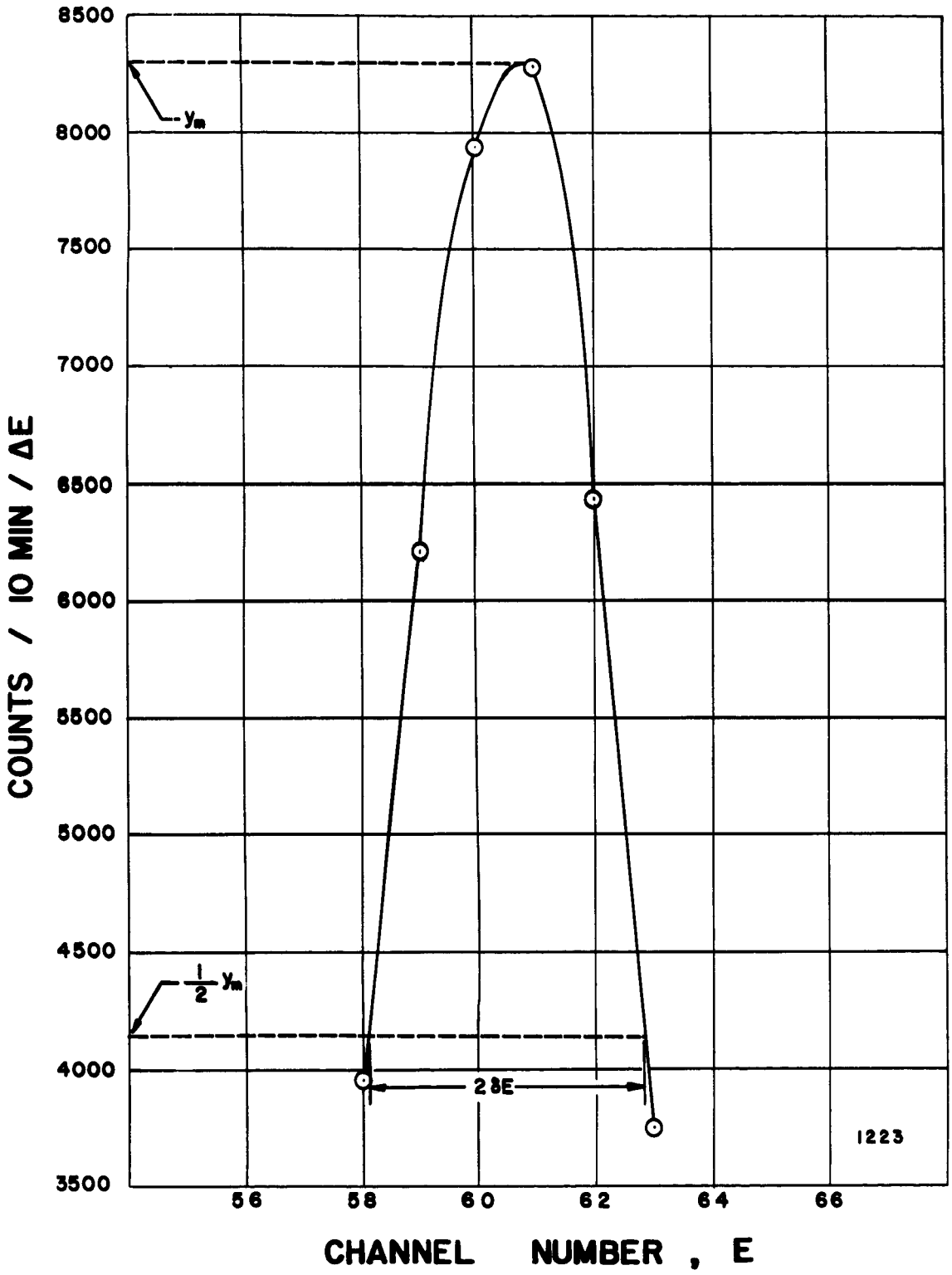

Figure 6A. 1.10 Mev Photopeak of Fe^{59} Retained on 10 Micron Filter.

y_m = 8289, and the area under the photopeak is:

$$P_{10\mu} = 2.13 \times 8289 \times \frac{4.70}{2} = 4.15 \times 10^4 \quad \frac{\text{counts}}{10 \text{ min.}}$$

and in milligrams:

$$W_{10\mu} = 4.15 \times 10^4 \, C = 4.15 \times 10^4 \times 2.415 \times 10^{-6}$$

or:

$$W_{10\mu} = 0.1 \text{ mg}$$

In percentage:

$$\frac{0.1}{5.31} \times 100 = 1.89\%$$

Finally, the photopeak corresponding to the 2 micron filter debris is shown in Figure 7-A. From here: $2\delta E = 8.9$, and $y_m = 47$. Hence:

$$P_{2\mu} = 2.13 \times 47 \times \frac{8.9}{2} = 4.46 \times 10^2 \quad \frac{\text{counts}}{10 \text{ min.}}$$

In milligrams:

$$W_{2\mu} = 4.46 \times 10^2 \times 2.415 \times 10^{-6}$$

or:

$$W_{2\mu} = 1.075 \times 10^{-3} \text{ mg}$$

and in percentage:

$$\frac{1.075 \times 10^{-3}}{5.31} \times 100 = 0.02\%$$

The results of the above calculations are summarized in Table IV-A, where also the percentages passing through, and retained by the different filter sizes, are indicated. It was assumed here that no debris passed through the 2 micron filter.

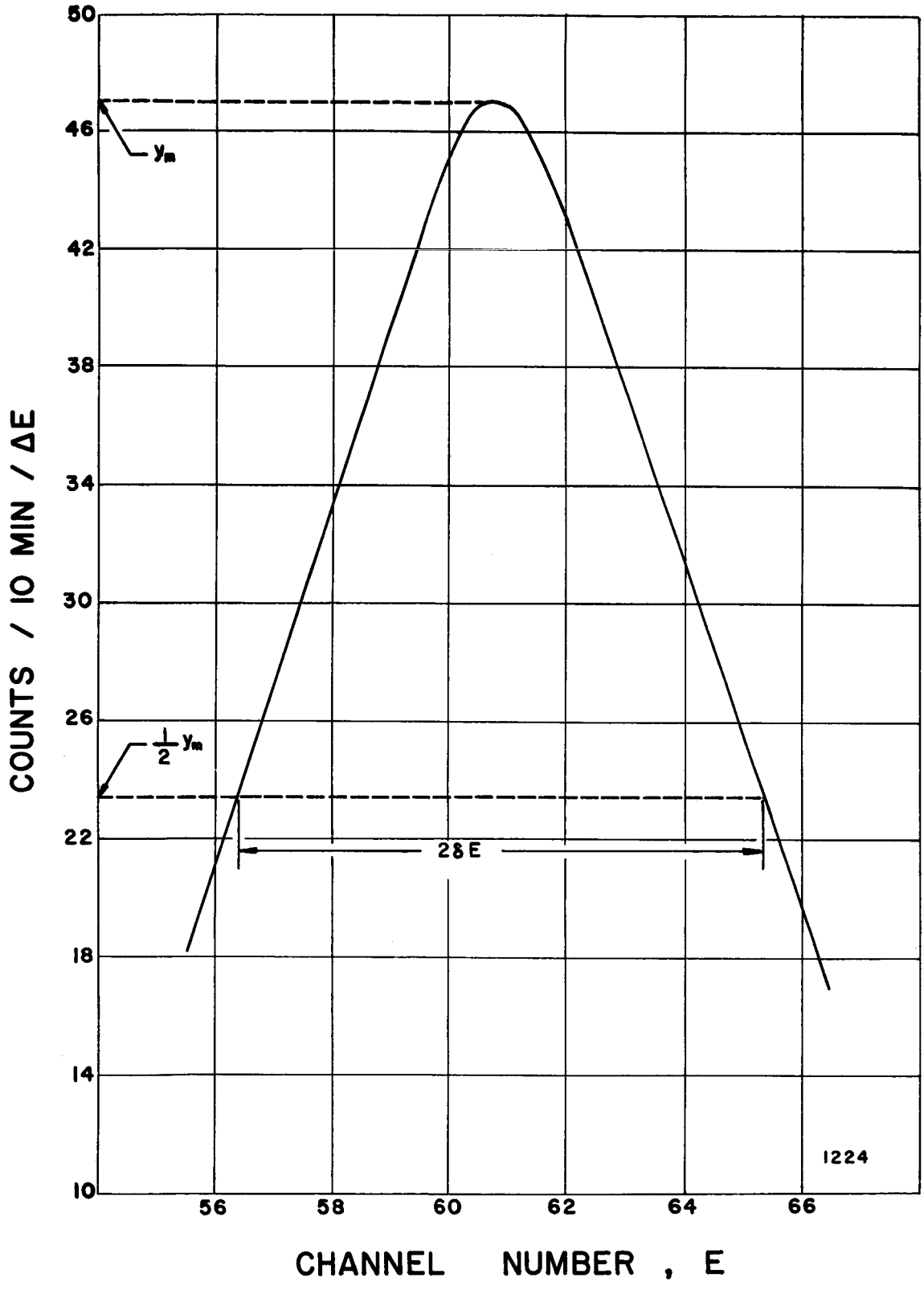

Figure 7A. 1.10 Mev Photopeak of Fe^{59} Retained on 2 Micron Filter.

TABLE IV-A

Percentage of Debris Retained and

Passing Through the Different Filters

Pore size (microns)	% Recovered (of Total Weight Loss)	Weight Recovered (mg)	% Retained In Filter	% Passing Through Filter
53	4.22	.224	68.95	31.05
10	1.89	.100	30.75	0.307
2	0.02	.001	0.307	0
Totals	6.13%	.325		

2. Particle Size Distribution

An estimate of the particle size distribution is performed now on the basis of the following assumptions:

i) The particles are spheres of diameter D. This diameter is selected to be 53 micron for the debris retained in the first filter, and an approximate average between the pore size specifications for the other cases. The reasons for this assumption are explained in the text.

ii) The size distribution in the amount of debris recovered (which is only 6.13% of the total weight loss) is identical to the size distribution of the particles not recovered.

iii) The density of the particles is uniform. For a steel with 99% iron and 1% carbon, this density[14] can be assumed to be $\rho = 7.83$ grams/cm^3.

Let N be the number of particles of a given diameter D. Then:

$$\frac{\pi}{6} D^3 N \rho = 0.00531 f$$

where f is the fraction retained in the filter of the corresponding

pore size, and the diameter is expressed in centimeters.

Hence:

$$N = 3.186 \times 10^{-2} \frac{f}{\pi D^3 \rho}$$

For the 53 micron filter, f = 0.6895 and:

$$N_{53\mu} = \frac{3.186 \times 10^{-2} \times 0.6895}{\pi \times (53 \times 10^{-4})^3 \times 7.83} = 6000$$

The diameter for the particles retained on the 10 micron filter is assumed to be an approximate average between 53 and 10 microns: D = 30 microns. For this case, f = 0.3075 and:

$$N_{30\mu} = \frac{3.186 \times 10^{-2} \times 0.3075}{\pi \times (3 \times 10^{-4})^3 \times 7.83} = 14,750$$

Finally, for the particles retained on the 2 micron filter, a diameter of 6 microns is assumed. Here, f = 0.00307 and:

$$N_{6\mu} = \frac{3.186 \times 10^{-2} \times 3.07 \times 10^{-3}}{\pi \times (6 \times 10^{-4})^3 \times 7.83} = 18,400$$

It is observed that, although the amount by weight retained in the 53 micron filter is the largest, the number of particles increases with decreasing size.